REGULATION OF RETINAL ACTIVITY IN AN *EX-VIVO* GUINEA PIG MODEL BY EXPERIMENTAL CONDITIONS AND EFFECTS OF ISOFLURANE AND PROPOFOL ANESTHETICS

by

Leah M. Wood

Submitted in partial fulfilment of the requirements
for the degree of Master of Science

at

Dalhousie University
Halifax, Nova Scotia
October 2010

DALHOUSIE UNIVERSITY

DEPARTMENT OF CLINICAL VISION SCIENCE

The undersigned hereby certify that they have read and recommend to the Faculty of Graduate Studies for acceptance a thesis entitled "Regulation of Retinal Activity in an *Ex-vivo* Guinea Pig Model by Experimental Conditions and Effects of Isoflurane and Propofol Anesthetics" by Leah M. Wood in partial fulfilment of the requirements for the degree of Master of Science.

Dated: October 21, 2010

Supervisor: _____

Readers: _____

_____

_____

DALHOUSIE UNIVERSITY

DATE: October 21, 2010

AUTHOR: Leah M. Wood

TITLE: Regulation of Retinal Activity in an *Ex-vivo* Guinea Pig Model by Experimental Conditions and Effects of Isoflurane and Propofol Anesthetics

DEPARTMENT OR SCHOOL: Department of Clinical Vision Science

DEGREE: MSc CONVOCATION: May YEAR: 2011

_____

Signature of Author

To my friends and family for your
unwavering patience, love and encouragement
since the beginning of my studies.

Table of Contents

List of Tables

List of Figures

Abstract

Electroretinoraphic signals (ERGs) are affected when recorded under isoflurane anesthesia in the operating room. We explored the effect of isoflurane and propofol in *ex vivo* guinea pig retinal preparations using a multielectrode array to record simultaneously ERGs and retinal ganglion cell (RGC) activity. The viability and light-response characteristics of the model were documented. In the presence of isoflurane, the ERG and RGC activity was reduced in a dose-dependent manner, even at sub-clinical doses; the OFF responses were consistently more affected. Propofol had minimal effects: at subclinical doses, a small excitation was measured while a concentration a hundred times stronger than the clinical concentration was required to measure a significant decline in EGR and RGC signals. This study confirms the usefulness of the guinea pig model to study clinically relevant retinal issues and shows that propofol is a better anesthetic to use in the operating room when retinal investigations are required.

List of Abbreviations and Symbols Used

ABR	auditory brainstem response
ACh	acetylcholine
Ag	silver
AgCl	silver chloride
AMPA	α-amino-3-hydroxyl-5-methyl-4-isoxazole-propionate
cGMP	cyclic guanosine monophosphate
CNS	central nervous system
CP_{50}	blood concentration of anesthetic required to prevent movement in 50% of the population
DA	dark adaptation
GABA	gamma aminobutyric acid
HPbCyD	2-hydroxylpropyl-b-cyclodextrin
ISI	inter-spike interval
K^+	potassium
LA	light adaptation
LED	light-emitting diode
LGN	lateral geniculate nucleus
MAC	minimum alveolar concentration
MEA	multielectrode array
MEP	motor evoked potential
mGluR6	Metabotropic glutamate receptor
N_2O	nitrous oxide
NMDA	N-methyl D-aspartate
O_2	oxygen

OR	operating room
PSTH	peristimulus time histograms
RGC	retinal ganglion cell
SCN	suprachiasmatic nucleus
SEP	somatosensory evoked potential
TTX	tetrodotoxin
VEP	visual evoked potential

Acknowledgements

My university career and this thesis would not have been possible without the support and mentorship from numerous individuals both from within the university and outside of it. I would like to extend my heartfelt gratitude to each of you.

- I would like to start by thanking my supervisor, Dr. François Tremblay for your patience, guidance, advice and motivation throughout my entire MSc degree. By allowing me to make and discover my own mistakes, you have given me the gift of realizing my own potential. You have enriched my growth as a student and researcher and inspired me to expand my horizons in new areas of vision science. Your insights on not only scientific areas but toward life in general have driven me to accept new challenges both academically and career related that I may have never considered if it were not for your encouragement. I am indebted to you in more ways than you know.

- Thank you to all the members of the Laboratory of Retina and Optic Nerve Research for you support and valuable input. It is with great sadness that I leave you all. A special thank you to Janette Nason for your everyday help and contribution to this project.

- Thank you to the faculty of the Clinical Vision Science program for providing me with the skills and confidence to always strive to "exhibit excellence" both academically and in clinical practice.

- I would like to extend my gratitude to my thesis supervisory and examining committee members for your assistance, suggestions and time.

- Thank you to the Nova Scotia Health Research Foundation for the studentship award provided during the execution of this project.

- A sincere thanks to all my friends from Acadia and Dalhousie for all the adventures, laughs, good times but most of all, just for being there.

- Finally, I would like to thank my family: Mom, Dad, Kayla, Melanie, Emily, Katelyn, Aunt Joan, Aunt Claire, Aunt Karen, Aunt Brenda, aunts, uncles and cousins for always believing in me and for your constant reminders not to take life too seriously. To my parents, words cannot express how much I appreciate all the sacrifices you have made to get me where I am today. This would not be possible without you. Mom, thank you for your unwaivering love, patience and understanding and for reminding me over and over again that everything will be OK in the end.

CHAPTER 1: INTRODUCTION

1.1 Presentation of Problem

1.11 Clinical Perspectives and Ground Work

Electroretinography (ERG) is a non-invasive clinical diagnostic test that measures the electrical activity emanating from the retina when it is flashed with light. It serves as a tool to evaluate the functional integrity of the retina and plays a fundamental role in the diagnosis of various retinal diseases. In most cases, a reliable ERG recording can be attained in a clinical setting and requires only minimal cooperation from the patient; however, the use of a large contact lens electrode is necessary to reduce the signal to noise ratio in the ERG signal (Gjotterberg, 1986). In specific cases, however; the invasiveness and discomfort caused by the corneal electrode can decrease patient compliance particularly in pediatric and special needs populations. In such situations, it can be necessary to consider performing the ERG under sedation or general anesthesia to obtain appropriate recording conditions (figure 1) (Tremblay & Parkinson, 2003).

Tremblay and Parkinson (2003) have documented detrimental modifications to the ERG signal when anesthetic agents are used. This is clearly demonstrated in figure 2 which shows human photopic ERG's recorded in an awake and cooperative child (top), under chloral hydrate sedation (middle) and under isoflurane anesthesia. The first two columns illustrate the ERGs and oscillatory potentials (OPs) recorded in a patient following a period of dark adaptation. The ERG of the conscious patient clearly shows two early (ON-associated) waves along with a third peak (associated with the OFF system). A minimal non-statistically significant reduction in amplitude of mostly the third wave is measured under chloral hydrate sedation, while the ERG recorded under

isoflurane anesthesia showed a severely disturbed signal with a significantly delayed and attenuated OFF component. The second column depicts the fact that the late OPs (OP4 and OP5) also underwent a reduction in amplitude and delay in implicit time under isoflurane anesthesia. Similar effects can be noted in the recordings obtained after a period of light adaptation.

The effects of halogenated anesthetics such as isoflurane on human ERGs remains a controversial topic as some reports state that isoflurane produces no effect (Debrabant, Hache, Cantineau, & Scherpereel, 1984;Wongpichedchai, Hansen, Koda, Gudas, & Fulton, 1992), or a decreased amplitude of the b-wave without a delay in implicit time (Tashiro et al., 1986).

For one clinical case at the IWK electrodiagnostic laboratory, an ERG was to be performed under anesthesia, however; an operating room was not available. Due to the fact that the test needed to be performed in a clinical setting instead, the anesthesiologist on the case decided that it may be more appropriate to use propofol anesthesia as it would be safer approach in this case. The recordings obtained under propofol anesthesia are shown in figure 3. As can be appreciated, the cone ERG wave morphology obtained under propofol anesthesia is much closer to what is expected in awake conditions (refer to figure 2, top traces).

The modifications that occur as a result of anesthetic and sedative agents on the ERG can hinder the ability of clinicians to interpret the signal and make an appropriate diagnosis. Given these clinical impacts and conflicting reports in the literature, it is imperative to work toward providing an accurate description of the actions of these anesthetics on the ERG signal. On those premises, it was thus decided to further study the

effects of anesthetics in an *ex vivo* animal retinal model.

1.12 Purpose of the Study

The purpose of this study is to investigate the impact of anesthetics on the ERG signal and retinal ganglion cell (RGC) activity using well-controlled experimental animal models. In order to accomplish this, it is also necessary to determine a suitable animal model and to test the viability of the *ex-vivo* retinal preparation. Based on previous clinical findings, we propose that isoflurane will be detrimental to both the ERG and RGC activity while propofol will have less of an impact on the retinal output.

1.13 Animal Models

Rodent (rat and mouse) animal models are the most commonly used animals in electroretinography research. While the scotopic ERGs of these animals are quite similar to those seen in humans, their photopic ERGs differ significantly. The photopic ERG recordings of rats and mice do not show an a-wave and the b-wave found in the rodent ERGs are much larger in amplitude than seen in human ERGs. The implicit time of the retinal potentials (ERGs and OPs) are also more delayed in rodents than in humans (Racine et al., 2005). Based on these differences, it is necessary to investigate another potential animal model to better represent the human photopic ERG.

Racine, et al. (2005) demonstrated that humans and guinea pigs share a similar a/b wave ratio, OP composition, timing and frequency domain. Human ERGs also demonstrate the photopic hill phenomenon in which at lower light intensities the amplitude of the b-wave increases as the luminance increases until a maximum point. Once it has reached this maximum level, the b-wave amplitude will begin to decrease as the light intensity continues to increase. This phenomenon may occur due to the

summation of the a- and b-wave field potentials (Wali & Leguire, 1992). Racine, et al. (2005) were able to demonstrate that the guinea pig ERG does follow this same trend with an increase in light intensity.

In addition, Lei (2003) demonstrated that the guinea pig long duration light stimulus photopic ERG demonstrated a positive OFF component similar to what is seen in humans and primates. In contrast, ERG expression of the OFF system in rats is through negative components.

Guinea pig retinas do have a similar structure to mammalian retinas; however, their retinal vasculature does differ significantly. In the human retina, chroroidal circulation provides oxygen (O_2) to the outer retinal layers, while retinal circulation provides O_2 to the inner layers. In contrast, guinea pigs do not possess an intraretinal circulation system. In fact, their retinas are completely avascular and the only source of O_2 delivery is through the choroidal circulation system.

Guinea pig retinas are indeed much thinner than human retinas. Retinal thickness had previously been assumed to be correlated with choroidal O_2 penetration distance in avascular retinas; however, one study showed that O_2 levels in the inner retinas of guinea pigs is actually quite low despite having a similar peak O_2 level in the choroid to that seen in vascularized retinas (Yu, Cringle, Alder, Su, & Yu, 1996).

Rats and mice are altricial animals due to the fact that they are born with their eyes closed; whereas, guinea pigs like humans are precocial animals and are able to open their eyes at birth. In precocial animals, most of the retinal development occurs in utero. The formation of the outer segment of photoreceptors and synapse creation occur before birth, allowing for adult like ERGs to be recorded immediately post-natal. In altricial animals,

only the inner and outer nuclear layers consisting of well differentiated ganglion cells and undifferentiated neuroblast cells respectively, are present at birth. Lastly, the retinas of precocial animals do undergo significant changes in both the cytoarchitectural structure of the tissue and function postnatal; however, to a lesser magnitude than seen in altricial animals (Racine, Behn, & Lachapelle, 2008).

1.2 Retina and Neural Tissue Characteristics

1.21 Retinal Tissue Organization

The human retina is a thin layer of tissue lining the back of the eye that contains neurons arranged in an intricate layered structure. Photoreceptors capture light photons and subsequently transmit that signal to second and third order neurons via pathways specific to individual components of the visual world (Heckenlively & Arden, 1991). The cell bodies of retinal neurons are located in one of three layers of the retina: the outer nuclear layer (ONL), the inner nuclear layer (INL), or the ganglion cell layer (GCL). Photoreceptors, namely rods and cones, have their cell bodies contained within the ONL and respond to individual light photons (Kolb, Fernandez, & Nelson, 1995). They subsequently transmit the light signal via a direct vertical pathway to bipolar cells located in the INL and then to ganglion cells located in the GCL. The synaptic interconnections between these neuronal cells occur in additional layers between the main nuclear layers referred to as the outer and inner plexiform layers (OPL and IPL respectively). In addition, two other types of cells are located within these layers that form horizontal surrounding interconnections with the neuronal cells of the vertical pathway. These cells are the horizontal cells (located within the OPL) and amacrine cells (located within the INL) and serve to provide lateral inhibition (Masland, 2001). The main vertical and

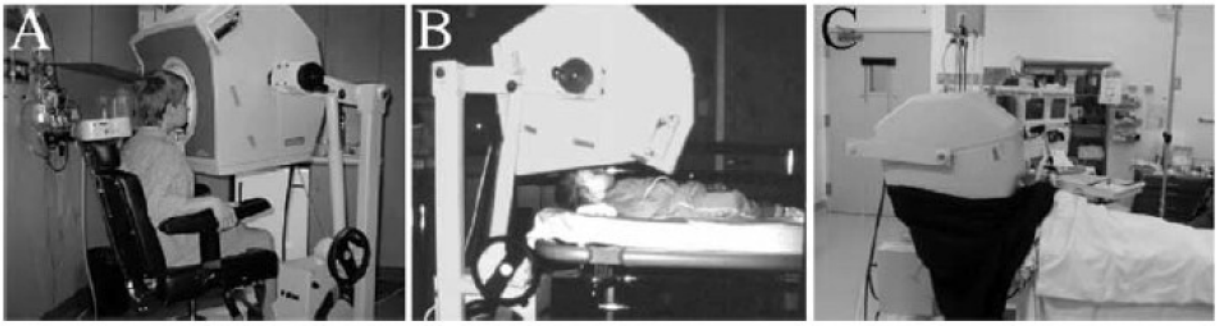

Figure 1. Examples of the set-up required for recording ERGs while the patient is awake, under sedation or under general anesthesia. Patients are sitting by themselves or on their parent's laps in front of the Ganzfeld (A). With sedation (B) or anesthesia (C), a supine position is adopted. In the operating room (C), the Ganzfeld and the patient's upper body is covered with a light proof drape, to create adequate conditions for dark adaptation (Tremblay & Parkinson, 2003).

Note. From "Alteration of electroretinographic recordings when performed under sedation or halogenate anesthesia in a pediatric population." by F. Tremblay & J. Parkinson, 2003, Documenta Ophthalmologica, 107, p.271-279.

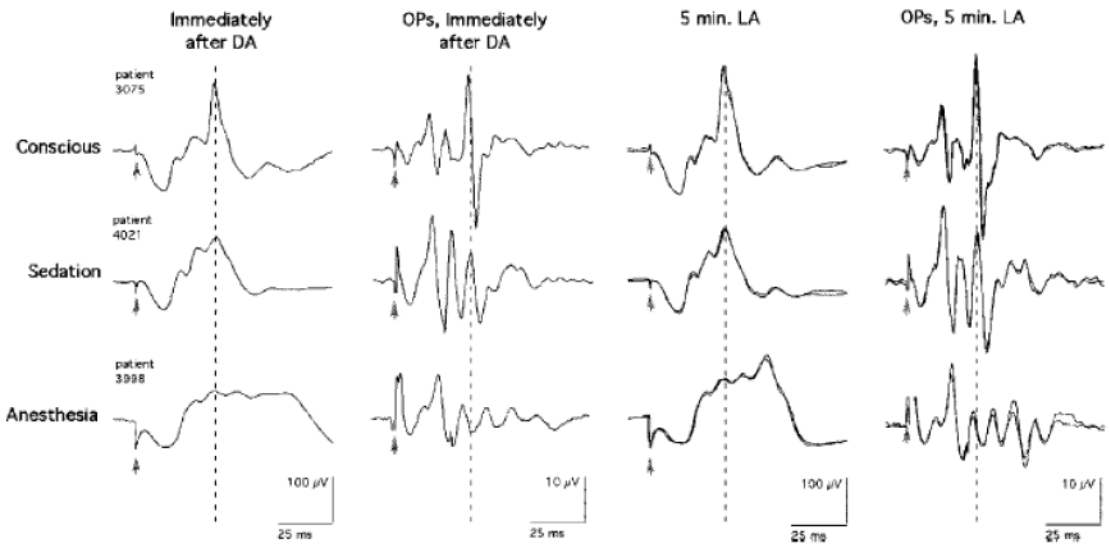

Figure 2. Representative ERG recordings obtained under photopic conditions in conscious (first row), sedated (second row) and anesthetized (third row) patients. The two first columns depict recordings obtained directly after a period of dark adaptation (DA) while the two last columns illustrate the same responses after 5 min of light adaptation (LA). The dash line is centered on the peak of the b-wave and of OP4 in the conscious patient recordings. Arrow: stimulus onset. Calibration indicated.

Note. From "Alteration of electroretinographic recordings when performed under sedation or halogenate anesthesia in a pediatric population." by F. Tremblay & J. Parkinson, 2003, Documenta Ophthalmologica, 107, p.271-279.

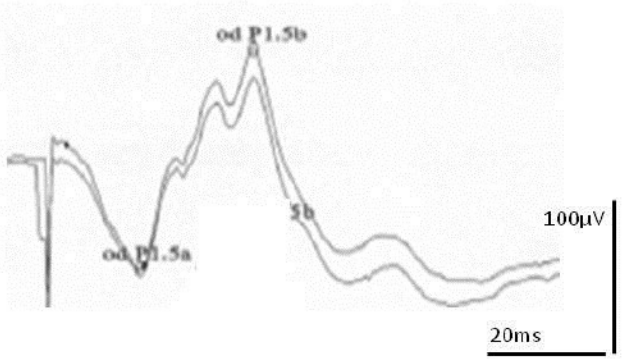

Figure 3. ERG recorded at the IWK Electrodiagnostic Laboratory with patient under propofol anesthesia in a clinical setting. The a-wave, b-wave and oscillatory potentials are clearly seen and are affected to a much lesser extent than when a patient is under isoflurane anesthesia.

horizontal pathways of the retina are outlined in figure 4.

1.22 Retinal Circuits

When the retina is exposed to light, it elicits a cascade of events that ultimately result in the generation of an action potential by the ganglion cells and the propagation of a nervous impulse to the visual cortex of the brain. This process involves the transmission of the visual signal through a series of retinal cells. It begins with the phototransduction of the photoreceptors followed by the delivery of the signal to the bipolar cells and ends with the generation of an action potential by the ganglion cells.

Photoreceptors contain photopigments that absorb photons of light. There are two types of photoreceptors: rods that respond to dim light and slow changes in illumination and cones that detect bright light and respond to fast changes in light intensity (Kolb, 2003). Light stimulation induces a series of biochemical events that ultimately result in a local change in ionic conductance of the photoreceptor outer segment membrane which alters the electrical potential of the membrane surface creating a slow, graded hyperpolarization of the cell (Baylor, 1987). Photoreceptors remain depolarized in the darkness, resulting in the neurotransmitter glutamate being released continuously in the dark and suppressed in the light (Kolb, 2003). These changes in electrical potential of the photoreceptors occur through a process called phototransduction.

Phototransduction involves a cascade of events that lead to the depolarization of the photoreceptors in dark conditions and hyperpolarization of the photoreceptors in light conditions. In the dark-adapted state, photoreceptors are partially depolarized due to an influx of sodium (Na^+) and calcium (Ca^{2+}) through open cyclic guanosine

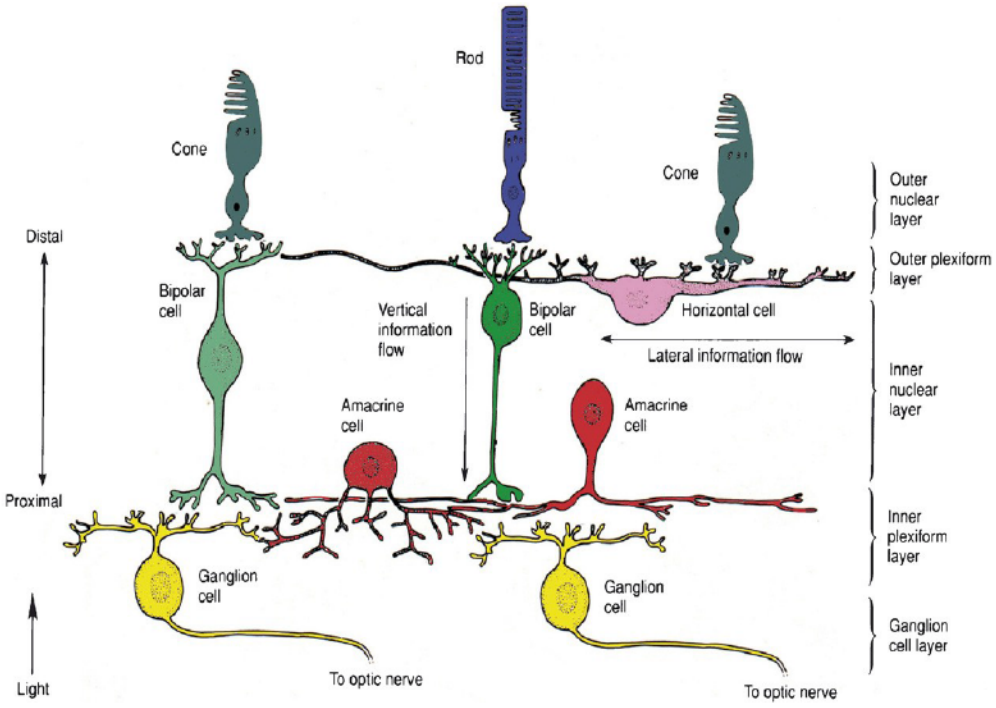

Figure 4. Schematic of the layers and neuronal cells of the mammalian retina. The incoming light (arrow on the lower left) passes through the whole retinal thickness before reaching the photoreceptors (rods and cones). The signal is then transmitted through the vertical pathway of visual information processing and influenced by the lateral neuronal connections.

Note. From "Physiology and pathology of somatostatin in the mammalian retina:A current view." by D. Cervia, G. Casini & P. Bagnoli, 2008, Molecular and Cellular Endocrinology, 286, p.112-122.

monophosphate (cGMP)-gated ion channels. An ionic balance is maintained through an ion exchanger and ion pump. The sodium/calcium-potassium (Na^+/Ca^{2+}-K^+) exchanger uses the sodium gradient to exchange Ca^{2+} and K^+ out of the photoreceptor, while an ATP dependant sodium-potassium pump removes Na^+ ions from the photoreceptor. During light absorption, the photopigment called rhodopsin contained within each photoreceptor undergoes a conformational change around the 11-cis bond forming all- trans retinal. This form of rhodopsin then binds and activates the G-protein transducin, which in turn, activates a phosphodiesterase that rapidly hydrolyzes cGMP. This results in a reduction of the intracellular cGMP concentration causing the cGMP-gated ion gates to close and prevent the influx of Na^+ into the photoreceptor. Since there is no change in the ion pump or exchanger, a negative change in membrane potential occurs and induces a graded hyperpolarization of the photoreceptor. The change in membrane potential of the photoreceptor triggers a reduction in glutamate release in the synaptic terminal of the cell (Heckenlively & Arden, 2006).

Photoreceptors relay visual information to the bipolar cells via glutamate release: in decreasing doses as light activation increases and in increasing doses as light activation decreases. The mature retina contains two types of bipolar cells: ON-type and OFF-type. ON and OFF bipolar cells make synaptic connections with photoreceptors in different layers of the IPL. The portion of the IPL containing the synaptic circuitry for the OFF cells is referred to as sublamina *a*, while the ON circuitry is found in sublamina *b* (Chalupa & Gunhan, 2004). ON-type bipolar cells depolarize with an increase in illumination, which plays a part in the detection of light images against a dark background. OFF-type bipolar cells depolarize when there is a decrease in illumination

and are conducive to detecting dark images against a light background (Kolb, 2003). OFF bipolar cells contain ionotropic glutamate receptors at their dendritic ending which respond to glutamate binding by opening voltage-dependent cation (Na^+,K^+, Ca^{2+}) channels. This subsequently leads to the graded depolarization of the cell. ON bipolar cells contain metabotropic glutamate receptors (mGluR6), which indirectly close voltage-dependent cation channels via a biochemical cascade (Westheimer, 2007).

Bipolar cells make synaptic contacts with both amacrine and ganglion cells. These cells synapse with amacrine cells mainly through two types of ionotropic glutamate receptors: NMDA (*N*-methyl *D*-aspartate) and AMPA (α-amino-3-hydroxy-5-methyl-4-isoxazolepropionic acid). In the human retina, rod bipolar cells mostly make contact with amacrine cells exclusively and do not make direct contact with ganglion cells. The signal from a rod driven ON bipolar cell is delivered to the AII cell, fed to the cone ON bipolar cell via gap junctions, and subsequently to the ON ganglion cell. In contrast, when the light stimulus is decreased, rod driven bipolar cells feed the signal via a glutametergic synapse to the AII cells where it is inverted through another inhibitory glycinergic synapse onto the cone OFF bipolar cell. From there, the signal is passed to the OFF ganglion cell. Cone ON and OFF bipolar cells release glutamate to signal the ON and OFF ganglion cells directly. Bipolar cells also possess sustained and transient Ca^{2+} currents that participate in forming tonic and phasic components of transmitter release to the third order neurons (Heckenlively & Arden, 2006).

Glutamate release from bipolar cells to the ganglion cells triggers the opening of voltage gated Na^+ channels and results in depolarization of the ganglion cell's dendrites. The resulting change in potential is integrated to elicit an excitatory post-synaptic

potential with saltatory conduction of the signal from the hillock of the RGC to the brain's visual center via the optic nerve. ON and OFF ganglion cells signals can further be classified as phasic (transient) or tonic (sustained) (Heckenlively & Arden, 2006). Acetylcholine (ACh) receptors, both muscranic and nicotinic types, have been documented to be associated with phasic ganglion cells of the retina, however; the effects of ACh on the mammalian retina are currently not well understood (Kolb et al., 1995).

The previously described vertical pathway that involves passing visual information from the photoreceptor to the bipolar cell and then onto the ganglion cells is further modulated by lateral interactions by horizontal cells and amacrine cells. Horizontal cells synapse with photoreceptors and bipolar cells in the OPL. They act to provide lateral inhibition by sending inhibitory signals to both the photoreceptors and bipolar cells contributing to visual integration (Remington, 2005). Amacrine cells synapse with bipolar cells and ganglion cells in the IPL. Several different types of amacrine cells serve to integrate, modulate and interpose a temporal domain to the signal that is passed from the bipolar cell to the ganglion cell (Kolb, 2003). Gamma aminobutyric acid (GABA) is the primary inhibitory neurotransmitter present in various types of large- field amacrine cells. It acts on bipolar cells, ganglion cells and other amacrine cells via their axons and cell bodies through three different kinds of GABA receptors (a, b and c) (Kolb, et al., 1995; Yu et al., 1996).

Lastly, three additional types of cells present in the retina are the Muller cell, astrocyte and interplexiform cell. The Muller cell is the primary glial cell of the retina and serves to maintain and provide structural support for the neuronal cells of the retina. Astrocytes are glial cells that enter the developing retina from the brain along the

developing optic nerve. They line ganglion cell axons and blood vessels of the nerve fiber layer forming axonal and vascular glial sheaths that make them a part of the blood-brain barrier. They may also serve as a nutritive service to neurons and play a role in ionic homeostasis by regulating extracellular potassium levels and metabolism of neurotransmitters such as GABA. In humans, the interplexiform cell is a GABAergic neuronal cell that links the IPL and OPL.

1.23 Visual System Organization

RGCs relay the visual output of the retina to the higher visual centers of the brain. RGC axons gather at the optic disc and give rise to the optic nerve which projects through a collagen network structure known as the lamina cribrosa. Once the optic nerve exits the lamina cribrosa, it becomes myelinated by oligodendrocytes. The optic nerve of each eye meets at a structure known as the optic chiasm that lies within the circle of Willis (an anastomosis of blood vessels). It is at this point that fibers from the nasal hemiretina cross to join temporal fibers from the temporal hemiretina of the fellow eye. In humans, approximately 90% of optic nerve fibers project along the optic tract and terminate in the lateral geniculate nucleus (LGN), whereas; the remaining 10% project to areas controlling pupil response or the circadian rhythm. The LGN is a layered structure in which the projections from each eye remain separated within individual layers. In primates, the two bottom layers are magnocellular layers while the upper four layers parvocellular. Each of these layers contains koniocellular sublayers. The LGN also receives input from cortical and subcortical centres along with reciprocal innervation from the visual cortex and serves as a center for complex processing. Axons leave the LGN as optic radiations and synapse onto the visual cortex where information is further processed (Remington, 2005).

A substantial amount of fibers from each optic tract bypass the LGN and project to the superior colliculus. This structure also receives visual input from the visual cortex.

Conversly, in rodents, greater than 95% of optic nerve fibers project to the superior colliculus with some fibers projecting to the dorsal LGN (Altman, 1962). Sparse amounts of fibers innervate the suprachiasmatic nucleus (SCN), the various nuclei of the accessory optic system, the hypothalamus and the inferior colliculus. Projections from that arise from the dorsal LGN project to the occipital cortex and the visual thalamic reticular nucleus for further processing (Kolb et al., 1995).

1.24 Molecular Structure of Membranes

The smallest basic unit of an organism is the cell. Cells contain outer membranes composed of a double layer of phospholipid molecules that separate their inner structures from the external environment. A phospholipid molecule contains a polar head that is hydrophilic and two long fatty acid chains are non-polar and lipophilic. The nature of these properties promotes the spontaneous arrangement of these molecules into a bilayer in aqueous medium with the polar heads directed outward and fatty chains lining the inside of the membrane. Transmembrane proteins are imbedded within the lipid bilayer. Their main purpose is to control the metabolic exchange with the internal cellular environment. Transmembrane proteins include energy-consuming pumps, carriers and ion channels (Lullman, Ziegler, Mohr, & Bieger, 2000). In some cases, specialized junctions physically join cells in order to promote cellular communication. One specialized type of junction is known as a gap junction, which allows only for the passage of small molecules and ions (Widmaier, Raff, & Strang, 2004).

In order for drugs to exert their actions, it is essential that they are able to permeate the lipid membranes to permit entry into cells, cell organelles and passage across the blood brain barrier. Substances can traverse lipid membranes in three different ways: diffusion, transport carriers and vesicular transport. Lipophilic substances can enter the cell by diffusing directly from the extracellular space through the membrane. Since many anesthetics are lipophilic, they may gain access to the cell by this method. Molecules that are not lipophilic can gain access to the cell via carriers; however, it is required that the substance has an affinity for the carrier. Finally, membrane penetration may occur with the help of transport vesicles that function by one of two systems: transcytosis and receptor-mediated endocytosis. The process of transcytosis involves a vesicle that is fused to the cell membrane. The vesicle engulfs substances dissolved in the extracellular fluid, breaks away from the membrane and carries the substance into the intracellular space. Once inside the cell, vesicles undergo fusion with lysosomes and the transported substance is subsequently metabolized. Receptor-mediated endocytosis begins when a drug binds to receptors on the surface of the membrane and signals proteins called adaptins. Subsequently, a number of drug-receptor complexes aggregate on a section of membrane that invaginates and engulfs the complexes to form a vesicle. Following a series of events inside the cell, the drug-receptor complex dissociates. The receptor is recycled and returned to the membrane while the drug binds to an endosome. The endosome then delivers its contents to its predetermined destination (Lullman et al., 2000).

1.3 Electroretinogram

The electroretinogram (ERG) is a diagnostic test that measures the electrical activity of the retina in response to light stimulation. The electrical activity is generated by radial currents that are caused by retinal neurons themselves or by changes in the extracellular potassium producing an effect on retinal glia. The ERG waveform is a field potential captured at the corneal level that is composed of the summation of several wave components and reflects the culmination of activity from all retinal cells. It is a reliable clinical tool that is fundamental for the evaluation of retinal health and it can be performed non-invasively with a corneal electrode under physiological or near physiological (anesthetic) conditions. When proper stimulus conditions are used, ERGs are useful in objectively detecting the activity of specific neurons in the retina (Heckenlively & Arden, 2006). The two main parameters used to measure the ERG are amplitude (size of wave peaks) and implicit time (timing of peaks) (Gouras, 1970). The type of ERG used in this study was a photopic Ganzfeld-ERG that is generated specifically by cone driven pathways in the retina.

The waveform elicited from the human ERG is representative of the summed electrical activity produced by several generators throughout the retina. In the photopic human ERG, the photoreceptor activity is associated with the negative a-wave. The cells of the inner nuclear layer namely the horizontal cells, amacrine cells, Muller cells and bipolar cells contribute in differing amounts to the subsequent positive peak known as the b-wave. The ganglion cell and optic nerve layer do not contribute to the ERG signal (Gouras, 1970), though this topic is still controversial (Bui & Fortune, 2004). Oscillatory potentials (OPs) are high frequency, low amplitude wavelets that are present on the

ascending limb of the b-wave. They occur as a result of both the rod and cone systems in response to a strong light stimulus (Heckenlively & Arden, 2006). Inhibitory feedback synaptic circuits in the IPL are thought to be the primary cause of these waves (Wachtmeister, 1998).

1.4 Anesthesia Primer

The modern definition of anesthesiology states that it is a medical practice that provides patients with insensibility to pain during surgical, obstetric, therapeutic and diagnostic procedures along with restoring and monitoring homeostasis post-operatively (Urban & Bleckwenn, 2002). There are three broad categories of anesthesia that aim at achieving this goal for various types of procedures. These categories include: general anesthesia, local anesthesia and topical anesthesia.

General anesthesia aims at producing three main neurobiologic effects: amnesia, hypnosis, and immobility (Solt & Forman, 2007). They can be administered by inhalation or injected intravenously. General anesthetics act on many tissues in the body via various molecular mechanisms, but most importantly, all anesthetics must pass through the blood-brain barrier in order to act on the neurons of the brain and spinal cord to produce these effects. Modern anesthetic techniques typically involve the co-administration of a hypnotic drug, analgesic drug and muscle relaxant to produce these three states. Single agent general anesthesia is rarely administered because all anesthetic agents have one or more undesirable side-effects. By administering them in combination, a smaller dose of each anesthetic can be used. It is the hope that undesirable effects of one drug can partially be eliminated by the opposite side effect of another drug (Urban & Bleckwenn, 2002). General anesthesics can be subdivided further based on their mode of action.

These categories include: halogenated, opioids, barbiturates, benzodiazepines and non-barbiturates.

Local anesthesia is used to prevent pain to a specific area by blocking impulses along specific central or peripheral nerve pathways. The effects of these anesthetics are reversible and complete return of nerve conduction follows the use of these drugs. There are two main types of local anesthetics based on their molecular structure: ester type and amide type. Some common examples of the ester type are cocaine, procaine, and benzocaine; while, lidocaine is a common amide type local anesthetic (Stoelting, 1999).

Topical anesthetics are applied directly to the skin or mucosal membrane to eliminate pain to the area during minor procedures in a clinical setting. They are fast-acting drugs that do not produce systemic side-effects unless delivered in very high doses. Topical anesthetics are available in creams, ointments, aerosols, sprays, lotions, and jellies. Their molecular structures are ester type and some common examples are cocaine, pontocaine and alcaine (Achar & Kundu, 2002).

For many years, scientists believed that all anesthetics exerted their effects through a common mechanism. Meyer and Overton discovered a strong correlation between anesthetic potency and the lipophility of anesthetic drugs (figure 5) (Urban, 2002). Their 'Lipid theories' infer a common action and non-specific mechanism associated with various anesthetics. Therefore, these theories point to membranes as the main action site of these anesthetics. It is suggested that they alter physiochemical properties of the lipid bilayer; thereby, inducing changes such as a thickening of the membrane, changes in the fluidity of phospholipids or alterations to ion channels resulting in reduced excitability of neurons. Although many anesthetic agents do follow

the Meyer-Overton correlation, modern research shows that lipid solubility is not the sole mechanism of action for all anesthetics. The surface and interior of the plasma membrane, lipid shell of integral proteins, hydrophobic pockets and amphiphilic surfaces of proteins have also been discovered as plausible binding sites for anesthetics. Others propose that polarity, size and rigidity of the anesthetic are also important factors in their actions (Grasshoff, Drexler, Rudolph, & Antkowiak, 2006).

The solubility of an anesthetic in blood can be quantified using the blood:gas partition coefficient, which is the ratio of the concentration of an anesthetic in the blood phase to the concentration of the anesthetic in the gas phase when the anesthetic is in equilibrium between the two phases. The blood:gas partition coefficient governs the rate of absorption and elimination of the anesthetic in the body. A low blood:gas partition coefficient indicates a low solubility of the halogenated anesthetic in the blood which is favorable because it indicates a faster induction rate, more precise control over the anesthetic induction rate and a faster recovery (Malviya & Lerman, 1990).

1.41 Various Types of General Anesthetics

In clinically relevant doses, general anesthetic agents are able to achieve amnesia, hypnosis, and immobility through interactions with various molecular targets. General anesthetics can be divided into groups based on their chemical composition and molecular action. These categories include: halogenated, opioids, barbiturates, benzodiazepines and non-barbiturates (figure 6).

Halogenated anesthetics such as isoflurane, sevoflurane, desflurane and alkanes are commonly used in operating rooms because they are cost effective and easily administered. These anesthetics take the form of volatile liquids and their chemical

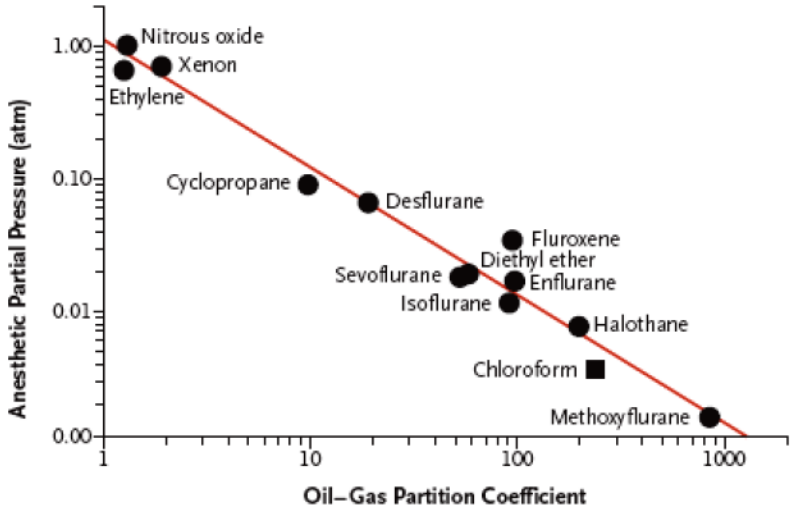

Figure 5. Meyer-Overton correlation. Graph of the oil-gas partition coefficient versus inhaled anesthetic partial pressure required to prevent movement in response to surgical incision in humans. This plot shows a strong correlation between the anesthetic potency and hydrophobicity of the anesthetics as referred to by the Meyer-Overton rule. Although most anesthetics follow this rule, it fails to explain the lack of anesthetic potency of some related hydrophobic compounds.

Note. From " Mechanisms of actions of inhaled anesthetics." By J.A. Campagna, K.W. Miller, D. Phil, S.A. Forman, 2003, The New England Journal of Medicine, 348(21), p.2110-2123.

structure includes an element (fluoride, bromide, chloride, etc) from the halogen group (group 17) of the periodic table (Solt & Forman, 2007). Halogenated anesthetics have a low solubility in blood, which is advantageous because it allows for rapid induction of anesthesia, permits precise control of anesthetic concentrations and prompts rapid recovery rates. At clinically relevant concentrations, these anesthetics are known to act on multiple molecular targets throughout the human body. Nitrous oxide (N_2O) is another commonly used inhaled anesthetic. It is an inorganic gas that is used in combination with other anesthetics (opioids or volatile anesthetics) and known for its analgesic properties (Stoelting, 1999).

Opioids are known for producing analgesia without the loss of touch, proprioception, or conciousness. The chemical structure of opioid anesthetics is made up of alkaloids of opium which can be separated into two categories: phenanthrenes and benzylisoquinolines. Some common phenanthrenes are morphine and codeine, while papverine and noscapine are representative benzylisoquinolines (Stoelting, 1999). Opioids may be natural or synthetic. Their mechanism of action involves acting as agonists at opioids receptor sites in the central nervous system and peripheral tissues (Stein, 1995).

Barbituates are defined as any drug derived from barbituric acid, which is a combination of urea and malonic acid. Some commonly used barbituates are pentobarbital and thiopental. The chemical structure of barbiturates results from substitutions on the number 2 and 5 carbon atoms of barbituric acid (Stoelting, 1999). Barbiturates interact with the GABA receptor to decrease the rate of dissociation of GABA from its receptor to prolong its inhibitory effects. They can also mimic the action

of GABA by directly activating chloride channels resulting in the hyperpolarization of the post-synaptic cell membrane and functional inhibition of the post-synaptic neuron.These anesthetics are known to produce sedative, hypnotic, hyperalgesic and anti-convulsant clinical effects; however, their use is very limited due to the availability of other more modern drugs with a better side effect profile (Kitahata & Saberski, 1992).

Benzodiazepines all share a benzene ring fused to a seven-member diazepine ring as the main component of their chemical composition. These drugs are known to induce varying degrees of sedation, anxiolysis, anticonvulsant actions, muscle relaxation and anterograde amnesia without impairing retrograde memory. These properties are beneficial for a variety of clinical uses but particularly for hypnosis the night before surgery, pre-anesthetic medication, and induction of anesthesia. Benzodiazepines act on $GABA_A$ receptors and induce increased affinity of the GABA receptor to the inhibitory neurotransmitter. Some examples of commonly used benzodiazepines are: diazepam, lorazepam, clonazepam, and midazolam among others (Ghoneim & Mewaldt, 1990).

The most frequently used non-barbiturate anesthetics in operating rooms include propofol, etomidate, and ketamine. Propofol and etomidate are intravenous anesthetics whose chemical structures are a substituted isopropylphenol and imidazole respectively. These drugs act on $GABA_A$ receptors to induce sedation and hypnosis; however, they are weak immobilizers (Solt & Forman, 2007;Vanlersberghe & Camu, 2008). Ketamine is a phencyclidine derivative that is considered to be a strong analgesic but weak hypnotic and immobilizer. It produces “dissociative anesthesia” in which the patient’s eyes remain open with a slow nystagmus present. Although the patient may appear awake, they are

non-communicative and varying degrees of skeletal muscle movements may occur. Ketamine is a potent blocker of NMDA receptors (Stoelting, 1999).

1.42 Halogenated Anesthesia

Frequently administered halogenated anesthetics in today's operating rooms are isoflurane, desflurane, and sevoflurane. These drugs are volatile liquids that are evaporated in devices known as vaporizers and administered to the patient as a vapor in an anesthetic circuit. Inhaling vapor into the lungs allows for rapid delivery of the anesthetic to the CNS because the anesthetics are quickly washed from the alveoli of the lungs to the brain via arterial circulation. This method allows for quick, easy and pain-free induction (Lerman & Jorh, 2009). Halogenated anesthetics can produce a variety of clinical effects at a range of concentrations due to their effect on multiple molecular targets, particularly ion channels. Inhaled anesthetics can induce amnesia, euphoria, analgesia, hypnosis, excitation and hyperreflexia. Higher concentrations cause deep sedation, muscle relaxation and diminished motor and autonomic reflexes to painful stimuli (Campagna, Miller, Phil, & Forman, 2003). The most common clinical scale used to measure the potency of halogenated anesthetics is the minimal alveolar concentration (MAC). The MAC unit refers to the minimum alveolar anesthetic concentration required to suppress movement in response to standard noxious stimuli in 50% of patients under controlled conditions (Eger, et al., 2008). The depth of anesthesia is also dependant on the solubility of anesthetic agents in the blood, namely the blood:gas partition coefficient.

Once in the alveoli of the lungs, halogenated anesthetics are carried to tissues and organs via the arterial blood stream. Distribution to the brain, liver, kidneys, and heart occurs more rapidly due to the high blood flow to these areas. Elimination occurs

primarily through the lungs and liver, while metabolites are excreted in the urine (Eggenberger et al., 2001).

This study will focus mainly on isoflurane anesthetic and its molecular targets and mechanisms of action.

1.421 Molecular Mechanisms of Isoflurane Anesthetic Action

Isoflurane (2-chloro-2-(difluoromethoxy)-1,1,1-trifluoro-ethane) is a halogenated methyl ether that exists as a clear, non-flammable liquid at room temperature and emits a pungent ethereal odor. It possesses extreme physical stability and does not undergo any detectable deterioration during 5 years of storage (Stoelting, 1999). Isoflurane has an intermediate blood:gas coefficient of 1.4 and a MAC of 1.15 vol% which allows for rapid induction and recovery.

Isoflurane is known to have an effect on many organs and systems throughout the body. It can cause a transient increase in heart rate, cerebral vasodilation, increased cerebral blood flow, and increased intracranial pressure. Isoflurane can also create respiratory irritation due to its pungency potentially leading to coughing, laryngospasm, breath holding, increased secretion, and oxyhemoglobin desaturation volume and increase in carbon dioxide pressure. Other possible side-effects associated with isoflurane are postoperative nausea and vomiting and rarely malignant hyperthermia (Stachnik, 2006). Lastly, halothane, a halogenated anesthetic similar to isoflurane, has also shown neuroprotective properties in light induced retinopathy by preventing the metabolic regeneration of rhodopsin and in turn protecting photoreceptors against apoptosis (Keller, Grimm, Wenzel, Hafezi, & Reme, 2001).

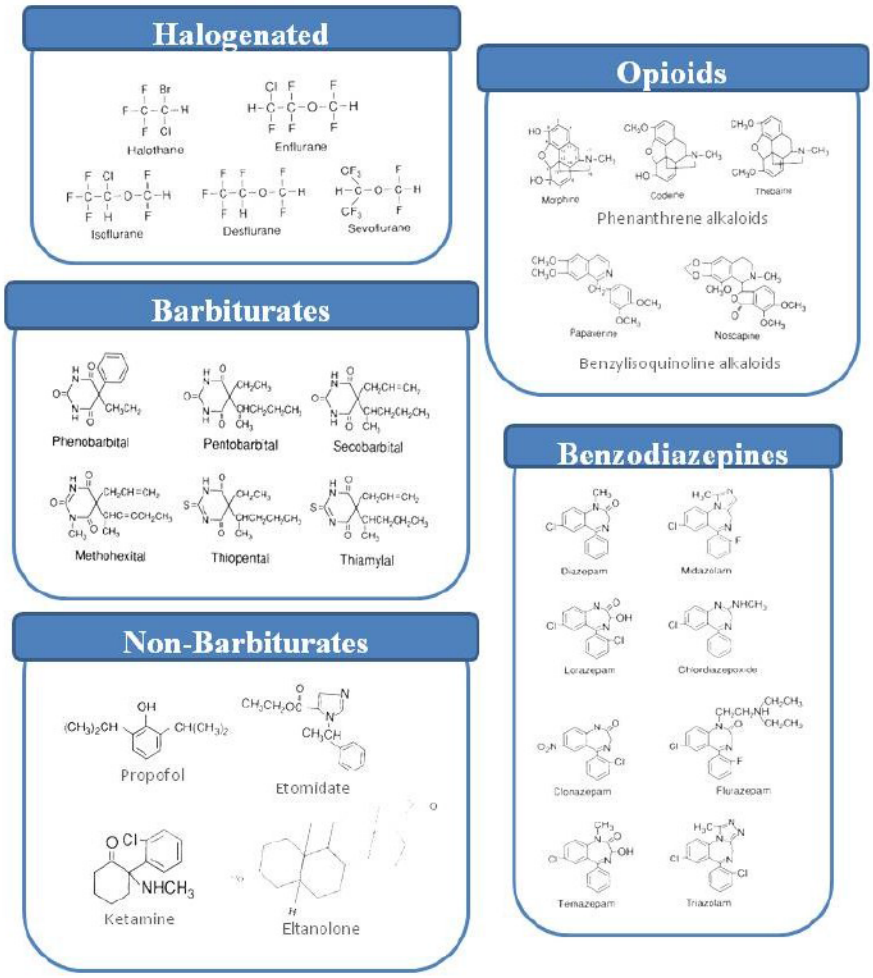

Figure 6. Classification of general anesthetics.

Note. Modified From " Pharmacology & Physiology in Anesthetic Practice." By R.K. Stoelting, 1999, Lippincott, Williams & Wilkins

Isoflurane exerts its molecular actions by selectively interacting with small cavities within most globular proteins. The proteins considered the most likely molecular targets of inhaled anesthetics are ion channels. The most prominently studied ion channels that are affected by inhaled anesthetics at clinically relevant concentrations are nicotinic acetylcholine, serotonin type 3 and $GABA_A$ (Campagna et al., 2003). Glycine receptors and glutamate receptors that are activated by NMDA and AMPA are also sensitive to halogenated anesthetics. Voltage gated ion channels such as sodium, potassium, and calcium channels can also influenced by these anesthetics; however, effects are usually only seen a higher than typical clinical concentrations. In addition, inhaled anesthetics are known to enhance inhibitory postsynaptic activity by acting on $GABA_A$ and glycine receptors and inhibit excitatory activity by acting on nicotinic ACh, serotonin, and glutamate receptors.

Isoflurane administration results in anxiolysis, sedation, amnesia, myorelaxation, and anti-convulsant activity by enhancing the ligand affinity facilitating the binding of GABA to its receptor (Stachnik, 2006). Isoflurane enhances the sensitivity of $GABA_A$ receptors to GABA and prolongs the inhibitiory currents in subsequent neurons (figure 7); however, the specific mechanism by which isoflurane impacts the receptor requires further investigation.

In addition to GABA receptors, isoflurane also potentiates and inhibits various other ion channels. Isoflurane enhances inhibitory glycine receptors, which contributes to decreasing spinal reflexes and startle responses. It also directly inhibits post synaptic NMDA and AMPA glutamate receptors affecting perception and memory. Serotonin type 3 receptors are also weakly affected inhibiting arousal of the patient; whereas, neuronal

ACh receptors are inhibited by isoflurane causing amnesia (Campagna et al., 2003). Lastly, isoflurane modulates voltage-gated calcium, potassium and sodium channels in order to contribute to decreasing neuronal excitability. The inhibition of calcium channels by isoflurane affects neurotransmitter release and affects the vascular tone, chronotropy and inotropy of the heart. Potassium channels play an important role in neuron recovery from action potentials; thereby, the inhibition of these channels by isoflurane can alter nerve conduction and cardiac action potentials (Campagna et al., 2003). Isoflurane is also known to affect sodium channels by interacting with the ion channel to produce a hyperpolarizing shift in voltage reducing its availability and recovery and to interact with open and resting sodium channels to produce a tonic block. These molecular mechanisms result in the inhibition of neurotransmitter release and subsequent action potentials (OuYang & Hemmings, 2007).

1.43 Intravenous Anesthesia

Intravenous anesthesics are injected directly into the blood stream via an intravenous (I.V.) infusion. They allow for rapid induction and maintenance anesthesia by continuous infusion pumps and permit a rapid recovery to an awake state. The principle pharmacological goal of intravenous anesthesia is to induce sedation and hypnosis via dose-dependant central nervous system (CNS) depression (Barash, Cullen, Stoelting, & Cahalan, 2009). These anesthetics are beneficial because they allow for minimal post-operative vomiting and a quiet and peaceful recovery (Lerman & Jorh, 2009).

In order to determine the correct dosage of intravenous anesthetic, the anesthesiologist must consider the pharmacokinetic (the body's disposition to a drug) and pharmacodynamic (therapeutic effect of the drug) differences between individual patients.

The potency of intravenous anesthetics can be defined by the arterial blood concentration required to prevent movement in 50% of the population (CP_{50}) (Andrews, Leslie, Sessler, & Bjorksten, 1997). Administration directly to the blood stream allows for rapid induction of anesthesia along with rapid delivery of the drug to the CNS and major organs (heart, kidneys and liver) because these tissues are highly perfused by the blood stream. The drug is also distributed to peripheral tissues at a rate that is dependant on blood flow to these tissues. The rate of diffusion to these tissues depends on the lipid solubility while anesthetics must be nonionized in order to pass through neuronal membranes. Most intravenous anesthetics undergo hepatic metabolism and water-soluble byproducts are eliminated via renal excretion (Barash et al., 2009).

The classes of intravenous anesthetics include barbituates, benzodiazepines, and non-barbituate anesthetics (etomidate, ketamine and propofol). This study will focus specifically on the molecular mechanisms of propofol.

1.431 Molecular Mechanisms of Propofol Anesthetic Action

Propofol is a substituted isopropylphenol (2,6-diisopropyl-phenol) that elicits sedation and hypnosis and is administered in an aqueous solution consisting of soybean oil, glycerol, and purified egg phosphatide. It is a highly lipophilic substance that allows for quick induction as a result of its rapid delivery to the CNS and is most often infused continuously to maintain anesthesia. The arterial blood concentration of propofol that is required to prevent movement in 50% of the population (CP_{50}) is 14.3µg/ml. Propofol also has a faster recovery than other intravenous anesthetics (Andrews et al., 1997). A high proportion of patients will experience pain during the injection of propofol due to the soybean oil included in the mixture (Trapani, Lopedota, Franco, Latrofa, & Liso, 1996);

therefore, it is occasionally combined with an inhaled anesthetic or prior injections of lidocaine or short-acting opioids (Stoelting, 1999). A combination of propofol and 2-hydroxylpropyl-β-cyclodextrin (HPβCyD) is currently being investigated as a potentially acceptable formulation to improve the water solubility of the drug and potentially increase patient tolerance to its parenteral administration (Trapani et al., 1996).

Propofol is known to have many pharmacological organ effects. It induces some cardiovascular depression resulting in a decrease of arterial blood pressure. Secondly, it is known to decrease cerebral blood flow and cerebral metabolic rate in a dose-dependant fashion (Vanlersberghe & Camu, 2008). Propofol has also been shown to reduce ventilation and potentiate hypoxic pulmonary vasoconstriction (Vasileiou, et al., 2009). Lastly, studies on the modulation of various aspects of inflammatory response have been performed. Some studies indicate that propofol decreases the secretion of proinflammatory cytokines, alters the expression of nitric oxide and impairs monocyte and neutrophil functions; however, this topic continues to be debated (Shibakawa, et al., 2005). The antioxidant properties of propofol are partly attributed to cardioprotective and neuroprotective effects that have been demonstrated in animal models (Vanlersberghe & Camu, 2008).

The principle mechanism of action through which propofol exerts its sedative and hypnotic effects is by enhancing GABA binding at the $GABA_A$ receptor. Propofol can reversibly potentiate the amplitude of membrane currents evoked by locally applied GABA in bovine cells (Hales & Lambert, 1991). It also prolongs synaptic currents mediated by $GABA_A$ receptors enhancing their inhibitory effect. Propofol slows the desensitization of $GABA_A$ receptors, which facilitates the rapid activation of inhibitory

synapses (Bai, Pennefather, MacDonald, & Orser, 1999). Furthermore, the effect of propofol is also concentration-dependant. Low concentrations of propofol potentiate the action of GABA at the $GABA_A$ receptor while moderate concentrations directly activate channel opening (Hara, Kai, & Ikemoto, 1993). Propofol also inhibits GABA uptake, which results in GABA accumulation in the synapse and may also contribute to its anesthetic effects (Vanlersberghe & Camu, 2008). Lastly, propofol increases the efficacy of piperidine-4-sulphonic acid, which is a partial agonist of $GABA_A$ receptors and helps to explain how propofol facilitates receptor opening (O'Shea, Wong, & Harrison, 2000).

Propofol is mainly GABAergic; however, it also exhibits effects on other sites of action as well. The inhibitory glycine receptors have been shown to be sensitive to propofol in spinal neurons (Hales & Lambert, 1991). Some excitatory NMDA glutamate neurons are also inhibited by propofol; albeit, with varying sensitivities. It also affects ACh release in select areas of the brain (frontal cortex and hippocampus) and inhibits sodium channels in human brain cortex tissue leading to reduction in the fractional channel-open time (Vanlersberghe & Camu, 2008).

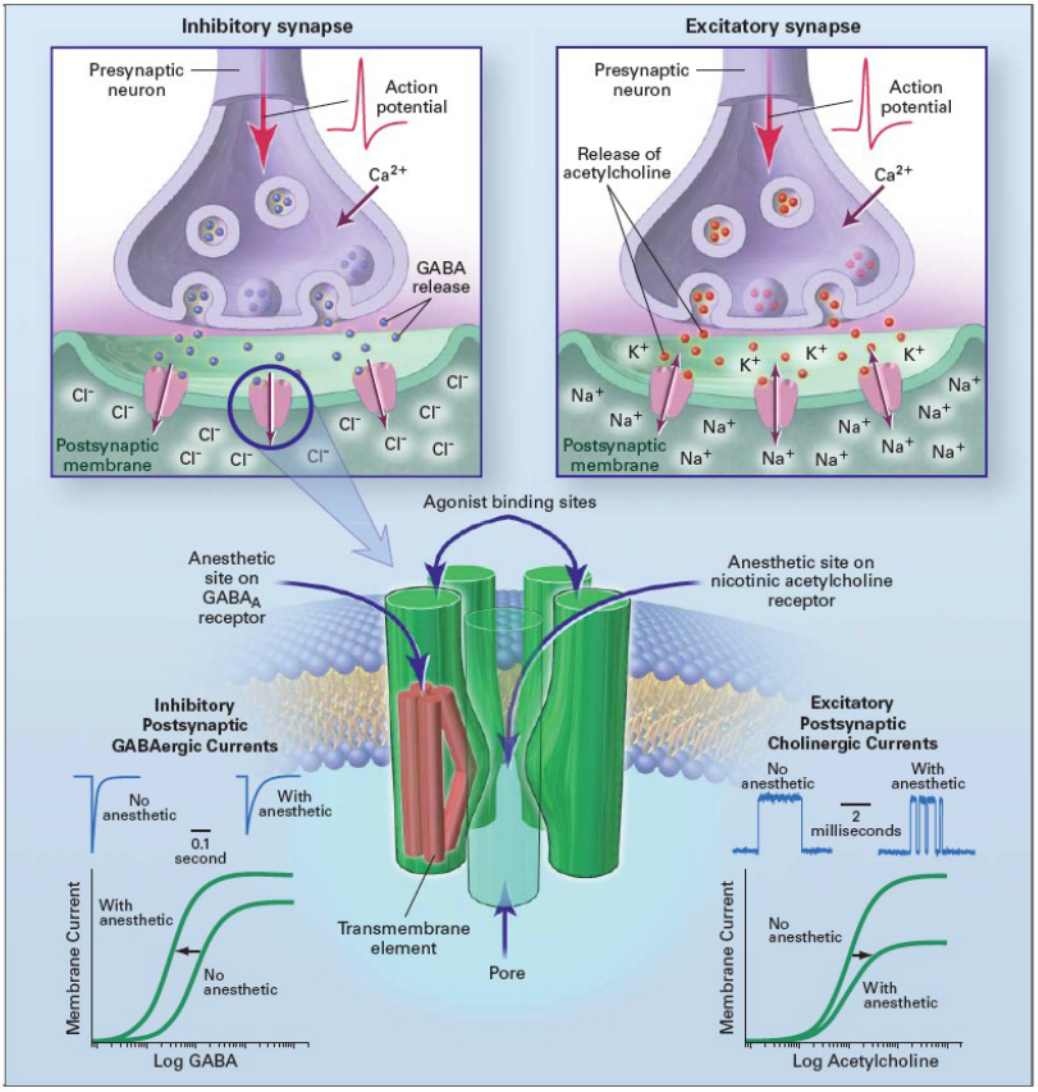

Figure 7. Schematic of an inhibitory and excitatory neuronal synapse. They are structurally similar but respond in opposite ways to anesthetic binding. The central figure depicts the anesthetic binding site on neurotransmitter receptor sites ($GABA_A$ and nicotinic ACh) on an ion channel that is imbedded in a lipid bilayer. Nicotinic ACh receptors are excitatory channels that depolarize on activation. Excitatory post synaptic currents activated by ACh are noncompetitively inhibited by anesthetics. $GABA_A$ receptors are inhibitory channels that once activated will hyperpolarize. Inhibitory post-synaptic currents are prolonged by anesthetics.

Note. From "Mechanisms of actions of inhaled anesthetics." By J.A. Campagna, K.W. Miller, D. Phil, S.A. Forman, 2003, The New England Journal of Medicine, 348(21), p.2110-2123.

CHAPTER 2: METHODS

2.1 Overview of Protocols

The effect of isoflurane and propofol anesthesia on the guinea pig retina were compared *in vivo* and *ex vivo*. In order to determine the impact of these anesthetics on the retina, ERGs and retinal ganglion cell (RGC) action potential activity were quantified.

In brief, *in vivo* ERGs were obtained in mice, rats and guinea pigs in order to determine the best animal model for human photopic ERGs. ERGs were then obtained in guinea pigs before and after isoflurane anesthesia and the results compared to the effects observed in humans.

Ex vivo recordings consisted of isolating retinae from a guinea pig eye cup. The collected retina was placed retinal ganglion cell side down in the perfusion chamber of an 8X8 multielectrode array (MEA) (30μm electrode diameter, 500μm spacing) and maintained at 38°C. The retina was superfused with an Ames solution and flashed with a long-duration light stimulus (LED 530nm, 500ms, 400 lux) to generate RGC action potentials. The retinal electrical activity captured by the MEA was bandpass-filtered to isolate ERG responses and windowed to isolated RGC spiking activity. After baseline recordings, isoflurane or propofol was delivered to the retina in various concentrations by introducing them into the perfusion system. Spiking counts of individual drug assays were determined using spike sorting software while ERG amplitude values were also recorded (figure 8). Several experiments were also performed in order to determine the viability of the *ex vivo* preparation.

2.2 Electroretinography

2.21 Animal Preparation

The animal subjects (guinea pigs, rats and mice) were kept on a 12 hour light/ dark cycle and housed cages with free access to food and water. The animal subjects were anaesthetized by an intramuscular injection of ketamine (90mg/kg; Bioniche, Belleville, ON)/xylazine (5mg/kg; Bayer Inc, Toronto, ON) and 1% cyclopentalate was administered to dilate the pupil. Normal body temperature was maintained by means of rectal temperature feedback. A drop of methylcellulose was given to each animal following which a DTL fiber electrode was placed on the cornea. Reference and ground electrodes were placed subdermaly in the forehead and hind leg of each subject, respectively.

2.22 Recordings

The guinea pigs, rats and mice were placed in front of a Ganzfeld (2503B Ganzfeld; LKC Technologies, Gaithesburg, MD) and an intensity-response series using various strength neutral density filters (Eastman Kodak Canada Inc., Toronto, ON)(flash intensity of 10 $cd \bullet s \bullet m^{-2}$, attenuated over 2 log units) was obtained in the presence of adaptive photopic backgrounds (2.8, 5.7, 9, 24, 42, 64, 110 and 170 $cd \bullet m^{-2}$). Full ERGs (1-300 HZ bandwidth 10K) and oscillatory potentials (OPs; 100-300 HZ bandwidth 50K) (PJII, Grass Instruments, Quincy, USA) were simultaneously acquired and averaged through LabView M5000 A/D card and dedicated software (National Instruments, Austin, TX). These ERG responses were then compared to human ERGs from a normative database compiled at the IWK Health Centre.

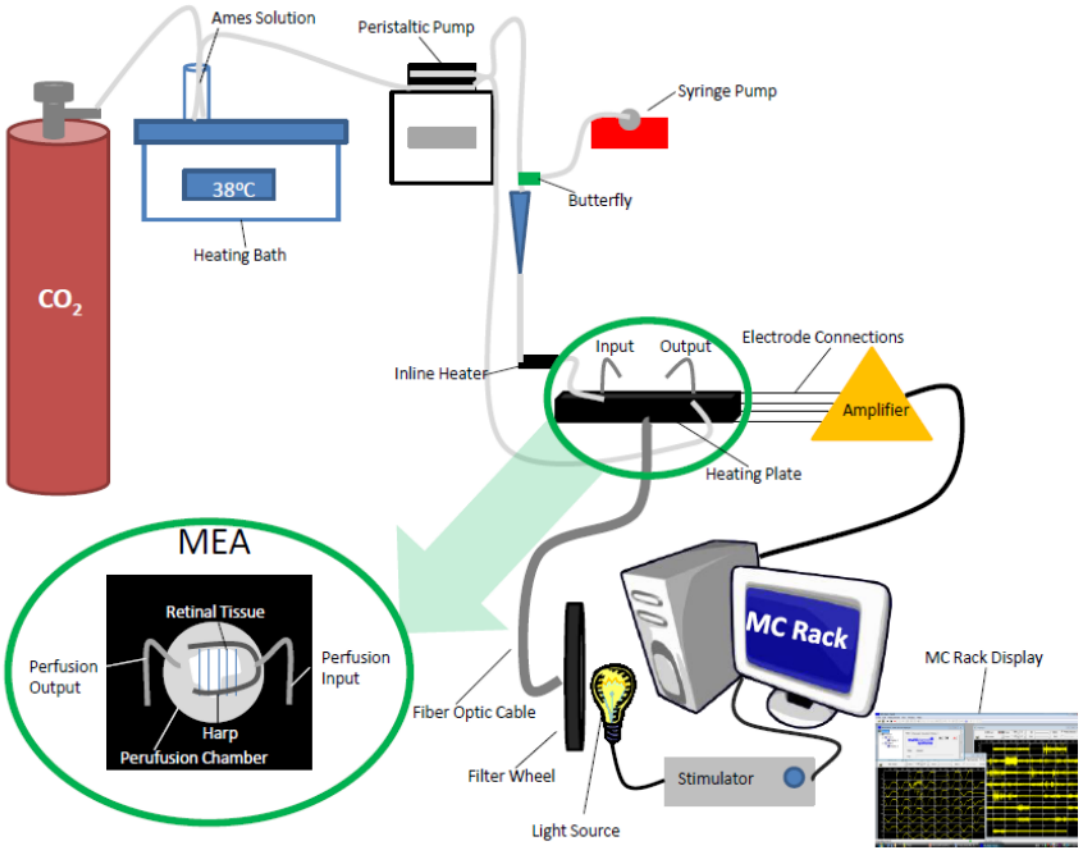

Figure 8. Schematic of the MEA set-up. A CO_2 tank is used to bubble prepared Ames solution that is heated to 38°C. A peristaltic pump delivers the Ames solution to the retinal preparation through tubing. The isoflurane solution is introduced into the perfusion system by means of a syringe pump. The MEA sits on a heating plate maintained at 38°C (zoomed in section). The retina sits on the electrodes RGC side down with a harp sitting on top of it. The Ames solution is circulated throughout the perfusion chamber by the input and output caniculi. The electrodes of the MEA connect to an amplifier that delivers the electrical output of the retina to the MC Rack software on the computer. The MC Stimulus software controls the light stimulus by means of the stimulator machine. A filter wheel is used to control the intensity of the light source that illuminates the retina via a fiber optic cable.

2.3 Multielectrode Array Recordings

2.31 Tissue Preparation

The guinea pigs were injected with Euthanyl (100mg/kg pentobarbitol; Bimeda-MTC, Cambridge, ON) in accordance with the weight of the animal. A cardiac puncture was performed once the guinea pig was no longer responsive to the pinch reflex. The eyes were then removed by elevating the eye with forceps and cutting the extraocular muscles and surrounding tissue. Following eye extraction, they were then transferred to a petri dish filled with Ames' solution at room temperature. The eye was perforated with a scalpel at the ora serata and micro-scissors were used to cut around the circumference of the limbus to release and remove the cornea and lens. The vitreous was removed with forceps and the retina was gently detached from the eyecup using forceps and a paint brush. The retina of one eye was transferred to a mesh-lined basket and suspended in bubbling Ames' medium maintained at room temperature as a backup. The second retina was placed ganglion cell side up on a piece of filter paper (Millipore, Billerica, MA) through which a small hole was punched in the centre. Any floating edges were flattened onto the paper with a paint brush. Lastly, the preparation was placed on the MEA RGC side down, heated to body temperature and perfused immediately with Ames solution.

2.32 Perfusion

The Ames medium was made by adding sodium bicarbonate (1.9g) to one liter of distilled water and bubbled with carbon dioxide (CO_2) for approximately 5-10 minutes. A bottle of Ames' medium (8.8g/L; Sigma-Aldrich, St Louis, MO, USA) containing L-glutamine was added to the solution and heated to 38°C. The pH of solution was tested with a pH meter (Denver Instruments GmbH, Göttingen, Germany) and adjusted with

sodium hydroxide (1N) until the pH settled between 7.4 and 7.5.

A perfusion chamber (diameter=26mm height=3mm) was centrally located around the MEA on top of which the retina was placed. A stainless steel horse-shoe-shaped harp was placed on top of the retina. An extra weight was also placed on top of the harp to further limit the movement of the retina. The Ames solution was delivered to the retina by means of 1/16 inch diameter polyethylene tubing connected to a Miniplus 3 peristaltic pump (Gilson, Inc., Middleton, WI). In order to insulate the preparation from the column of perfusa, a dripper was created using a syringe needle and a pipette tip. It was removed from the chamber via thin tubing that was also connected to the peristaltic pump. The Ames solution was delivered to, and removed from, the retina at a rate of 1.7ml/min after adjusting the level of the solution so that the retina was approximately 0.1mm below the surface. A silver/ silver chloride (Ag/ AgCl) grounding electrode was positioned toward the front of the chamber and allowed to contact the perfusion solution.

The isoflurane solution was created by adding approximately 20ml of isoflurane (AErran 1-5%; Abbot, Montreal, QC) to approximately 30ml of prepared Ames' medium and placed in a gas tight bottle. The solution was manually shaken to create a concentration gradient. The pH of the solution was measured using a pH meter and adjusted with hydrochloric acid until the pH settled between 7.4 and 7.5. A gas tight glass Hamilton syringe (Hamilton Company, Reno, NV) was used to extract approximately 2ml of the solution directly at the interface of isoflurane and Ames solution. The concentration at the interface was reported to be in the range of 13.4mM and 15.3mM (McDougall et al., 2008; McKenzie, Franks, & Lieb, 1995). The solution in the syringe was maintained at 38^{o}C throughout the experiment. Various volumes of the

isoflurane solution (0.1ml-1ml) were further diluted with Ames medium to create a 10ml total solution. The anesthetic was introduced into the perfusion system via a butterfly tubing that was connected to a larger syringe containing the drug. The syringe was placed in a syringe pump (Kent Scientific Corporation, Torrington, CT) that released the drug into the perfusion tubing at a rate of 1ml/min. The final MAC concentration of isoflurane was calculated using reported aqueous concentration (mMol) to MAC conversion factor for isoflurane (1MAC, 0.31mM) at 37°C (Franks & Lieb, 1996).

The propofol solution was prepared by dissolving 16.2g of 2-hydroxypropyl-β-cyclodextrin (HPβCyD) (Sigma-Aldrich Company, St. Louis, MO) into 100ml of distilled water in order to achieve a 16.2 (%w/v) solution. Propofol (2,6-Diisopropylphenol, 97+%) (SAFC Supply Solutions, St. Louis, MO) was added to this solution in excess in order to saturate the solution. The reported solubility of propofol in this saturated solution is 14.47± 0.42mg/ml (Trapani et al., 1996). The CP_{50} value for propofol in healthy women after skin incision is reported to be 14.3±1.6µg/ml (Andrew, Leslie, Sessler, & Bjorksten, 1997). Various volumes (5µl-1000µl) were diluted with Ames medium to create a 10ml total solution and mimic propofol concentrations less than, equal to and greater than the clinical blood concentration of propofol. The propofol solution was maintained at 37°C and bubbled with CO_2 for the duration of the experiment. The drug was introduced to the retina by circulating it throughout the perfusion tubing.

2.33 Multielectrode Array Description

A standard multielectrode array (Multi Channel Systems, Reutlingen, Germany) containing 60 electrodes in an 8X8 layout grid was used. The electrodes were made of titanium nitride and have a diameter of 30µm and interelectrode spacing of 500µm. Their

impedance can range between 30kΩ and 400kΩ. Tracks and contact pads are made of silicone with silicon nitride insulation material (Multi Channel Systems MCS GmbH, 2005).

The MEA was stored in distilled water at room temperature. Prior to each recording, it was placed in an ultrasonic cleaner (L&R Manufacturing, Kearnsay, NJ) with Teragazym detergent (Alconox, White Plains, NY) and then rinsed thoroughly with distilled water and dried carefully with kimwipes.

The MEA sensor is placed on the MEA preamplifier with blanking circuit (MEA-1060-BC-PA, Multi Channel Systems MCS GmbH, Reutlingen, Germany). The contact pins in the lid of the amplifier are pressed onto the contact pads of the MEA. The signal was then sent to the MEA filter amplifier with a gain of 1000 and bandwidth ranging from 0.1Hz-10kHz. The amplifier emited a signal to the data acquisition computer by means of a 68 pin MCS standard cable. The MEA system has a 50kHz sampling rate per channel. The analog output signals of the MEA amplifier are then acquired and digitized by the MC_card. In addition, the MEA amplifier also comes equipped with an integrated heating system that maintained the temperature of the MEA and was programmed by a temperature controller (Multi Channel Systems MCS GmbH, 2005).

2.34 Protocols

2.341 Baseline Over Time

A retina was mounted onto the multielectrode array and given 15-20 minutes to settle. It was then stimulated with long-duration light flashes (LED 530nm, 500ms, 400lux; Light Speed Technologies, Campbell, CA). Baseline recordings at 3 different light intensities (400 lux attenuated by 0, 1 and 2 log unit neutral density filters) and

spontaneous activity recordings of 65 sweeps in length were then taken every 30 minutes over a 2.5 hour period to monitor any baseline changes over time. When not recording, the retina was continuously stimulated with the light stimulus at the lowest intensity of 400 lux attenuated by 2 log unit neutral density filters.

2.342 Intensity Series

An MEA mounted retinal preparation was stimulated with a 500ms light stimulus over 8 light intensities (400 lux attenuated by neutral density filters in steps of 0.5 log units) after allowing the retina to settle for 15-20 minutes. Recordings of spontaneous activity were recorded continuously while the light intensity recordings were triggered 100ms prior to the light flash and ended 700ms post-light stimulus. All recordings were 65 sweeps in length.

2.343 Temperature-Response Relationship

A retinal slice was mounted on the MEA and given 15-20 minutes to settle once the perfusion was started. Baseline recordings (530nm, 500ms, 400lux) were acquired with the heating plate set at 38°C by the temperature controller (TC02, Multi Channel Systems MCS GmbH, Reutlingen, Germany). Recordings at various temperature intervals (36°C, 34°C, 32°C, 28°C) were then acquired with 4 minute time periods given between recordings to allow the retina to reach desired temperatures.

2.344 Dose-Response Relationships

Once the retina was mounted on the MEA and given 15-20 minutes to settle, baseline recordings were taken. The baseline recordings consisted of 65 sweeps at 3 light intensities (400 lux attenuated by 0,1 and 2 log unit neutral density filters controlled by a filter wheel). A spontaneous activity recording of 65 sweeps was also acquired during this

time.

Varying concentrations of isoflurane (0.43MAC to 4.32MAC) and propofol (5µg/ml-1000µg/ml) solutions were introduced to the retina by methods outlined in section 2.32. The retina was exposed to the drug for a period of 4 minutes before a recording at the brightest light intensity was taken. Once this recording was complete, regular perfusion was reinitiated while the remaining light intensity and spontaneous activity recordings were performed.

During recovery, the retina was continuously stimulated with light at the lowest intensity. After a washout of approximately 20-40 minutes, recovery recordings were taken at all 3 light intensities along with a spontaneous activity recording.

2.343 Constant Dose Time-Response Relationships

The isoflurane solution was created as described in section 2.32. After baseline recordings were taken, as described in section 2.341, 1 MAC of isoflurane solution was delivered into the perfusion system for varying periods of time by means of the syringe pump as described in section 2.32. The syringe pump was started and let run for a specific period of time (1min, 3min, 5min or 7min) and then a recording was taken at the brightest light intensity. After this recording, the syringe pump was stopped and the regular perfusion was reinitiated and the remaining recordings were acquired (2 light intensities and spontaneous activity).

During recovery, the retina was continuously stimulated with light at the lowest intensity. After a washout of approximately 20-40 minutes, recovery recordings were taken at all 3 light intensities along with a spontaneous activity recording.

2.35 Data Acquisition

The electrode raw data was recorded using the dedicated MC_rack software (Multi Channel Systems MCS GmbH, Reutlingen, Germany) and continuously stored on the hard drive of the computer.

Once recordings were complete, the replayer function of the MC_rack software was used to retrieve the data. High pass and low pass filters within the software were used to isolate RGC spiking activity and ERGs respectively from the electrode raw data. Thresholds were set for each individual electrode in such a way that the software could differentiate between RGC spiking activity and baseline noise. After the spiking activity was captured by the software, a windowing function was used to isolate individual RGC cells and a raster plot for the activity captured by individual electrodes was also created. Once all individual thresholds were set, an output file containing the filtered data for ERG and RGC action potentials was recorded and imported to Neuroexplorer software (Nex Technologies, Littleton, MA) for further analysis.

2.4 Data Analysis

2.41 Electroretinograms

2.411 *In vivo* ERGs

Ganzfeld ERGs and oscillatory potentials were simultaneously obtained *in vivo* from the guinea pig. This data was analyzed using Matlab software (The MathWorks Inc., Natick, MA). For the Ganzfeld ERG, the a-wave was calculated from the pre-stimulus baseline to the trough of the wave. The b-wave amplitude was measured from the a-wave trough to the largest positive peak. The implicit times of these waves were calculated by determining the exact timing at which the most negative or positive point of these peaks

occurred. The oscillatory potentials were also analyzed using the Matlab software in the same fashion to determine if there was a change in amplitude or implicit time between control and experimental conditions.

2.412 *Ex vivo* ERGs

The ERGs recorded *ex-vivo* were imported into the Neuroexplorer software and the post-stimulus time histrogram function was used to display of the average ERG waveform from each individual electrode. The numerical analysis function was then used to extract the maximum and minimum values from each channel within a set time range to determine the amplitude of the a-wave.

2.42 Action Potentials

2.421 Peristimulus Time Histogram

Standardized peristimulus time histograms (PSTHs) were constructed in order characterize the rate and timing of RGC actions potentials in relation to the light stimulus. In order to produce the PSTH, the retinal ganglion cell spiking activity that was recorded over a set number of sweeps was windowed and saved using the MC_rack software, and then imported into the Neuroexplorer software. PSTHs were created for individual cells using a bin width of 1 ms for the purpose of illustration (figure13, 15, 17, 22, 24 and 27) while a bin width of 0.1s was used for numerical analysis.

Subsequently, this data was exported to excel where the total number of spikes in individual bins were combined so that spike counts could be calculated for 100ms before the light stimulus, while the light stimulus was ON and while the light stimulus was OFF.

2.422 Inter-Spike Interval Correlograms

The inter-spike interval (ISI) correlogram is a graphical representation of variation

of time intervals between individual RGC spiking events (figure 29 and 30). It represents the correlation between the I^{th} interval and the $I^{th}+1$ interval between spiking events and serves as a measure of the regularity of the signal. The ISI correlograms were created using a dedicated application within Neuroexplorer software.

2.423 Statistical Analysis

Excel software (Microsoft Office 2008, Microsoft Corporation, Redmond, WA) was used to calculate averages of the total number of spikes occurring during 100ms pre-stimulus, for the 500 ms the light stimulus was ON and the 700ms the light stimulus was OFF for each anesthetic concentration. As several drug concentrations were tested on a single preparation, the spike count for the experimental condition was compiled for each experiment and normalized with the spike counts immediately preceding the experiment (return to baseline from previous experiment). The spike count was also used to determine the nature of the cell response; if the total number of spikes occurring during the ON segment of the stimulus was higher than the spike count in the OFF segment, the cell was classified as having an ON response (not necessarily as being an ON-center cell); the ratio of spike count ON/OFF was therefore superior to 1 if the cell responded with more spikes during the ON stimulus. Cells were also classified as phasic vs tonic if the ratio between the first 200 ms and the last 300 ms of the dominant response (either ON or OFF) was superior to 1. This information was then exported to Stata software (Stata Corporation LP, College Station, TX) for statistical analysis. ANOVA was used to study the effect of the anesthetics on ganglion spikes counts between varying concentrations of anesthetics. Paired t-tests were used to compare the effect of the anesthetics on ON versus OFF response for each drug trial. A sample t-test was used to determine if the normalized

ON and OFF responses differed from 1 (the control condition just preceding the experimental one). Scatterplot and bar-graphs were generated using the Excel software

2.5 Ethical Approvals

All experimental animal treatments were reviewed and approved by the Dalhousie University Committee on Laboratory Animals.

CHAPTER 3: RESULTS

3.1 Justification of Animal Model

Guinea pig, rat and mouse photopic Ganzfeld ERGs were carried out and compared with previously acquired human photopic ERGs in order to determine the appropriateness of the animal model chosen for this study.

OPs isolated from human, guinea pig, rat and mouse photopic average ERG traces from retinal recording are presented in figure 9. In human photopic ERGs acquired from the IWK Electrodiagnostic Laboratory, early and late OPs behave differently as the background intensity is decreased (figure10 I. b)). As the background intensity is dimmed, early OPs associated with the ON pathway increase in implicit time, while late OPs associated with the OFF pathway decrease in implicit time. The OPs of the guinea pig ERG (n=5) behave in the same fashion as illustrated in figure 9 II.b). In the rat (n=3) and mouse (n=3) models (figure 9 III.b) and figure 9 IV.b)), all OPs react the same way to a decrease in background intensity; therefore, early and late OPs cannot be segregated.

Secondly, the ERG signal obtained with a long duration light stimuli distinguish the guinea pig from the rat and mouse as demonstrated in figure 10. While humans and the guinea pig share a positive ERG response to the offset of the stimulus, the rat and mouse ERGs show negative components.

Figure 11 illustrates the *in vivo* photopic ERGs (1,3,5) and OPs (2,4,6) under the influence of 3% isoflurane for time periods of 1 minute and 10 minutes. The implicit time of the a-wave and OPs associated with the ON system remain stable during both isoflurane trials, while the implicit time of later OPs associated with the OFF system show some delay but no decrease in the amplitude.

3.2 Technical MEA Experiments

A total of 27 retinal preparations were retained for this thesis. A typical guinea pig retina placed on the MEA and maintained at 38°C under control conditions had an average of 70.8 ± 16.4 (mean± SD) RGCs being recorded simultaneously (range of 42-133), in our standardized conditions. A proportion of 52.4% ±14.3 responded preferentially to the offset of the stimulus, while 70.2% ±14.9 responded preferentially with a tonic response. ERG waveforms obtained *ex vivo* consisted of a single large negative peak with a mean amplitude of 0.17±0.012 mV.

MEA recordings were carried out to determine how experiment duration (n=4), variations of light intensity (n=6) and changes in temperature (n=3) influence the ERG and retinal output of an isolated guinea pig retinal preparation (scattergraphs in figure 12, ANOVA analysis in table 1).

Figure 12 1.a. demonstrates that the RGC action potential recordings that were triggered when the light stimulus was turned ON and OFF, along with the total spiking activity and spontaneous activity, did not decrease significantly over a 2.5 hour period of having the retinal preparation perfused on the MEA. This is confirmed by statistical analysis using ANOVA (table 1) and illustrated by the PSTHs of two representative cells from one retinal preparation in figure 13. The percentage of tonic versus phasic cell response types hovered at approximately 70%. In addition, the percentage of ON versus OFF cell response types also remained stable throughout the duration of the experiment (figure 12 I.c.). The average amplitude of the ERG was the only parameter showing a significant change over time (p=0.050). Post Hoc analysis shows that it was the ERG decline in the first 30 minutes of the experiment that was the main contributor to this

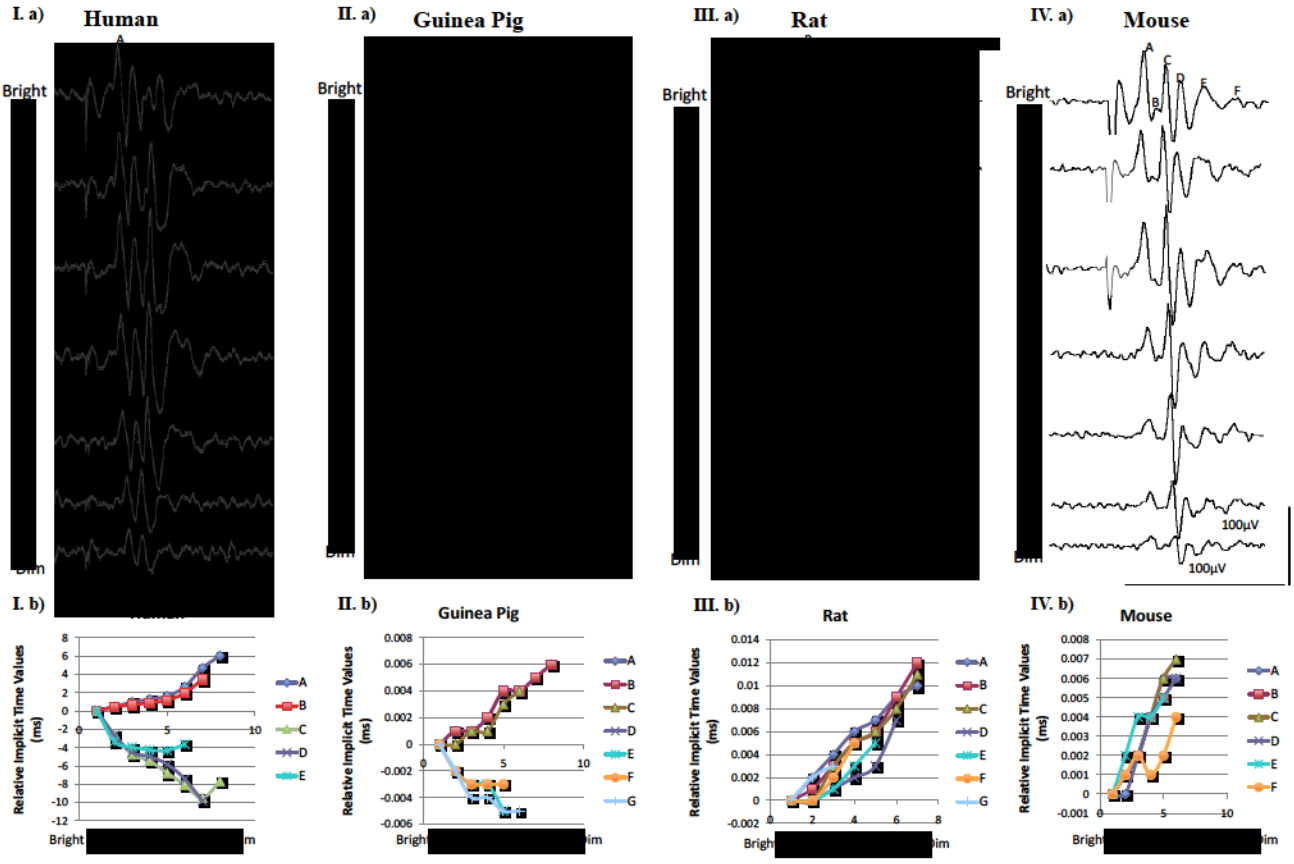

Figure 9. Oscillatory potential recordings acquired for several background intensities in the human (I. a)), guinea pig (II. a)), rat (III. a)), and mouse (IV. a)). The upper graphs illustrate the OPs collected from one representative animal, to series of background intensities (2.8, 5.7, 9, 24, 42, 64, 110 and 170 cd•m^{-2}). The lower graphs quantify the relative implicit time of individual OPs with changes in background intensity. The relative behavior between implicit time of early and late OPs discriminate the rat and mouse from the guinea pig and human.

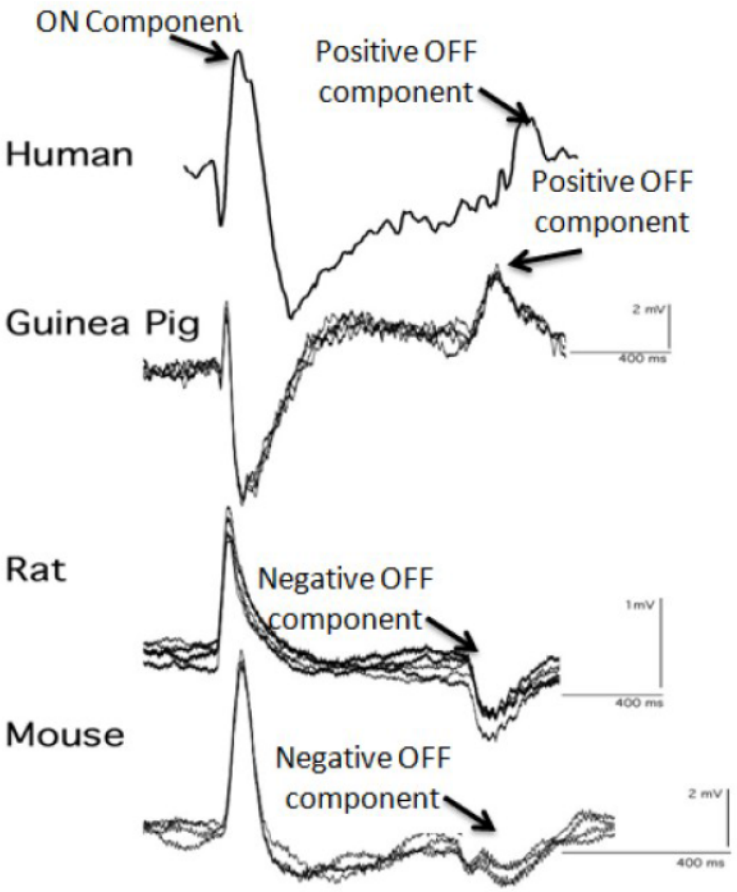

Figure10. Long-duration photopic ERG recordings from a human, guinea pig, rat and mouse. Calibration as indicated.

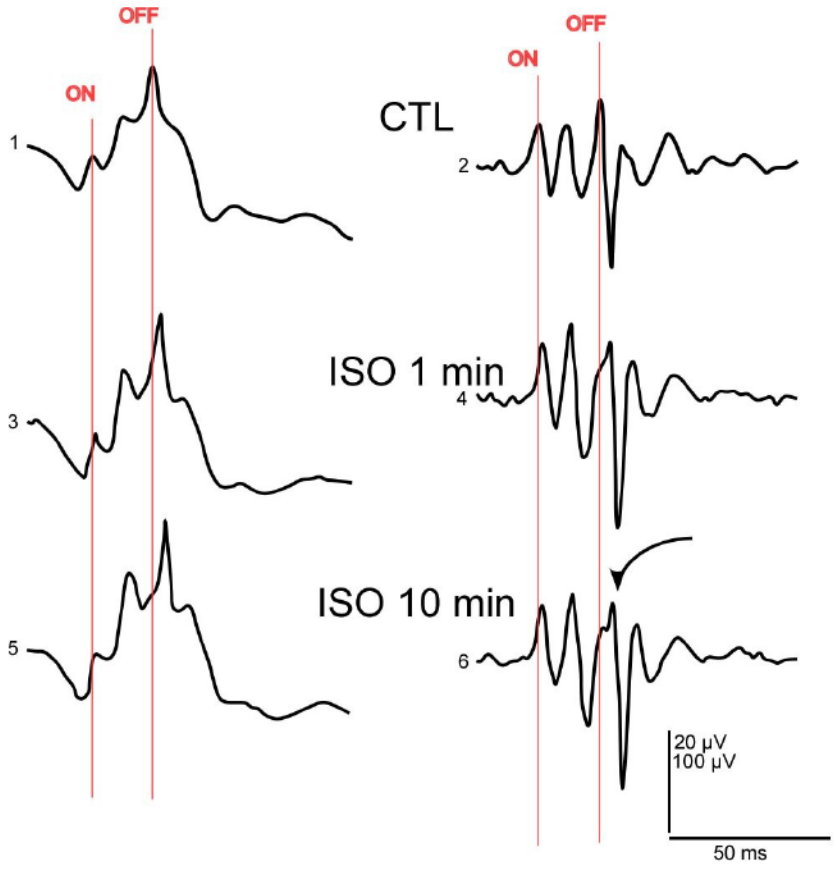

Figure 11. *In vivo* photopic ERG recordings (1,3,5) and OPs (2,4,6) from a guinea pig under the influence of 3% isoflurane (ISO) versus no isoflurane (control; CTL) for 1 minute and 10 minute time periods. The relative positions of the ON and OFF associated waves in control and isoflurane conditions are indicated by the red lines.

statistical significance. This is also depicted in figure 14 where the behavior of the averaged ERG from one MEA channel can be followed over time.

Varying light intensities also had an effect on the average number of RGC spikes and the ERG. As the light intensity was decreased, the average total number of spikes decreased significantly (p=0.000; table 1 third column) and as demonstrated by the PSTHs of two representative cells in figure 15. The number of spikes associated with the ON (p=0.000) and OFF (p=0.000) stimulus also followed this pattern; however, the spontaneous spiking activity did not decrease significantly with a change in light intensity (p=0.960) (figure 12 II.a.). The percentage of tonic responsive cells did not change significantly with variations in light intensity; however, the percentage of OFF responding cells did increase significantly (p=0.020) (figure 12 II.b.). Post Hoc analysis reveals that it was the sharp increase in the percentage of OFF responding cells at the dimmest light intensities from the baseline that mainly contributes to the statistical significance. Furthermore, the ERG amplitude decreased as the light intensity was decreased (p=0.000); however, it began to stabilize at the lowest intensities presented to the retina as demonstrated in both figure 12 II. c. and figure 15. The decline of activity of both the ERG and the RGC spiking activity followed a typical sigmoid curve that can be described by the Naka-Rushton equation ($V=V_m+(I^n/(I^n+K^n_{1/2}))$) (Susta, Stirn-Kranjc, Hawlina, & Brecelj, 2008). As both curves are normalized, the only parameter of interest is $K_{1/2}$, a semi-saturation constant that determines the sensitivity of the system. Interestingly, $K_{1/2}$ is much lower with the ERG signal; -1.44 log attenuation with the ERG, compared to -2.56 log attenuation for the RGC activity.

Lastly, the effect of changes in temperature of the MEA heating plate on the RGC spiking activity and ERGs was investigated. As the temperature decreased, there was a significant decrease in the total retinal output (p=0.003; table 1 fourth column and figure 12 III.a.) as is also illustrated in figure 17. Interestingly, there was a significant decrease in ON RGC responses (p=0.004) but not the OFF (p=0.110) or spontaneous RGC activity (p=0.850) with a decrease in temperature (figure 11 I.a.). Figure 12 III.c. and figure 18 demonstrate that there was an overall decrease in ERG amplitude (p=0.003) as the temperature was lowered. No significant changes in the percentage of OFF versus ON cells or tonic versus phasic cells was noted with changes in temperature (figure 12 III.b.).

3.3 Isoflurane Experiments

A concentration equivalent to 1 MAC of isoflurane was perfused to the retina for varying periods of time (n=5) in order to determine the amount of time necessary for isoflurane to produce its maximal effect on the retinal output. Figure 18 and figure 20 I.a. demonstrate that after 1 minute of exposure to isoflurane there was no significant change in the retinal output which is confirmed statistically by ANOVA analysis in table 2 (second column). Paired t-tests were used to compare the effect of isoflurane on ON versus OFF responses for each exposure time and reveals that there is no significant difference between both types of responses (figure 19). All experimental data has been normalized to the previous recovery because several doses were tested on a single preparation and recoveries are sometime incomplete or the health of the preparation can change over time. A sample T-test was used to compare the effect on total number of ON or OFF responsive RGC activity post anesthetic introduction as compared to the recovery of the previous experimental condition (figure 19 asterisk).

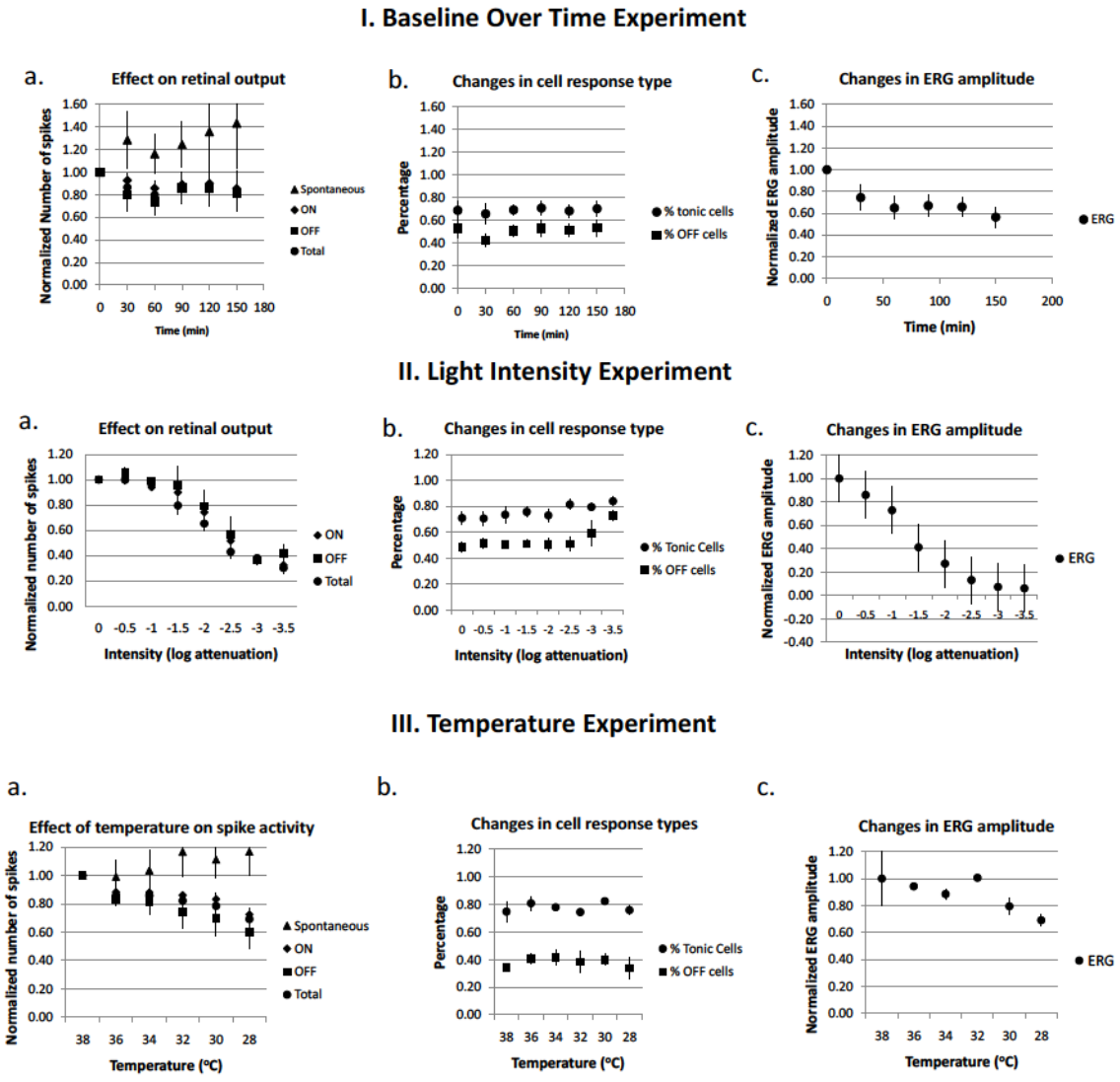

Figure 12. Effect of experiment duration (I), variations in light intensity (II) and changes in temperature (III) on RGC spiking activity (a), ON versus OFF and phasic versus tonic cell response types (b) and ERG amplitude (c). Graphs display data normalized to the initial baseline recordings.

Parameters	Baseline Over Time Experiment (n=4)	Light Intensity Experiment (n=6)	Temperature Experiment (n=3)
Effect on Total Retinal Output			
Spontaneous Activity	p= 0.870	p= 0.960	p= 0.850
ON response	p= 0.900	**p= 0.000**	**p= 0.004**
OFF response	p= 0.800	**p= 0.000**	p= 0.110
Total Response	p= 0.850	**p= 0.000**	**p= 0.003**
Type of Cell Response			
% Tonic	p= 0.990	p= 0.350	p= 0.650
% OFF	p= 0.850	**p= 0.020**	p= 0.870
ERG			
Amplitude	**p= 0.050**	**p= 0.000**	**p= 0.003**

Table 1. Statistical ANOVA table for technical experiments. ***p*<0.05**

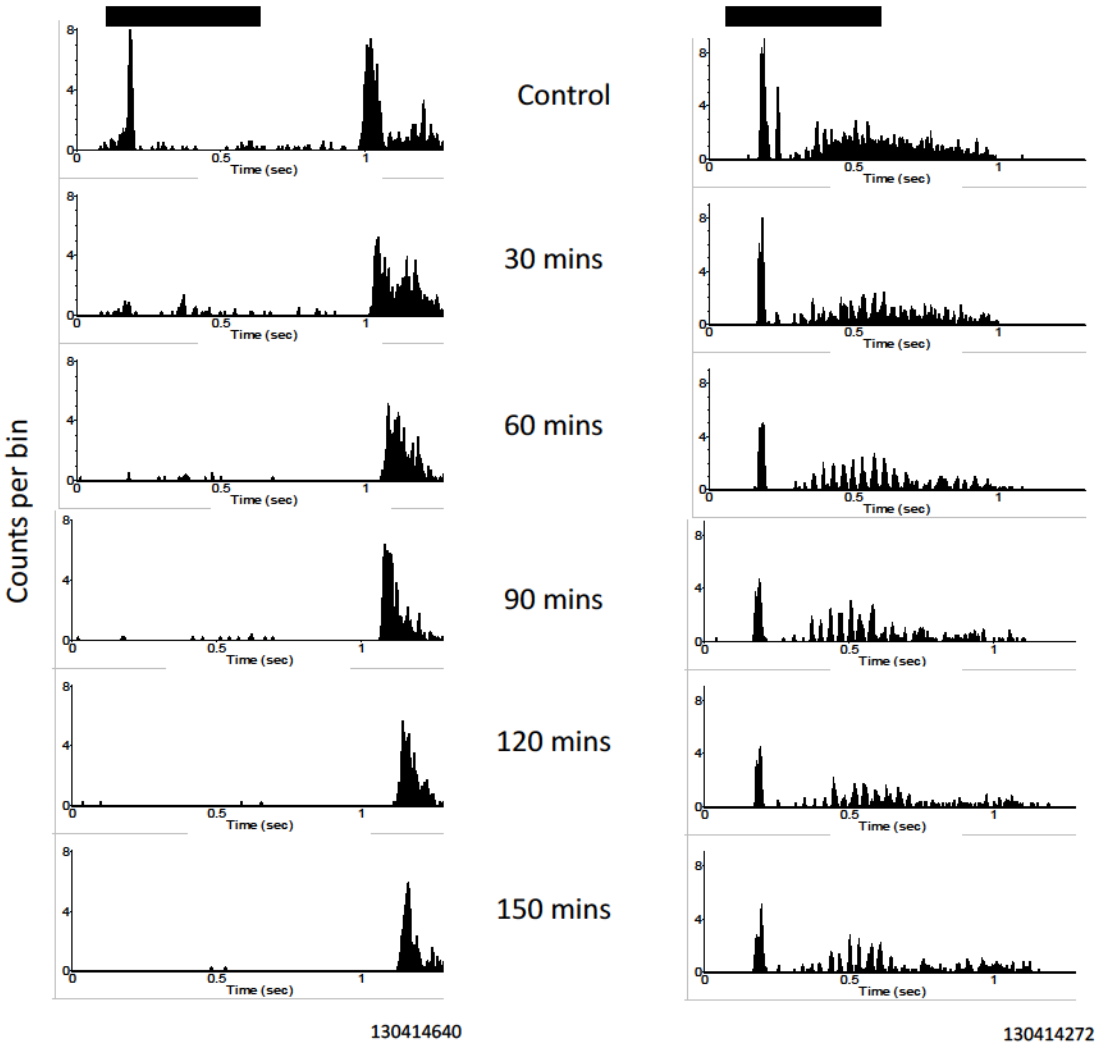

Figure 13. Effect of experiment duration on RGC spiking activity of individual cells. Two series of PSTHs from two cells recorded simultaneously from the same retinal preparation, illustrating the effect of experiment duration on RGC spiking activity.

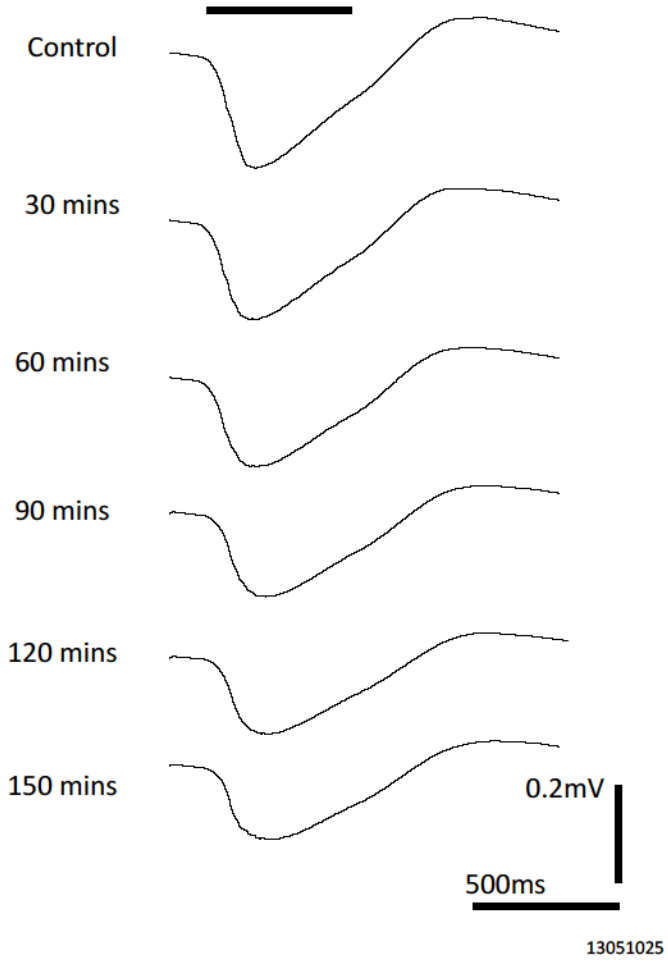

Figure 14. Effect of experiment duration on the ERG. Illustration of the average ERG collected from one MEA channel from a retinal preparation that was maintained on the MEA for a period of 2.5 hours.

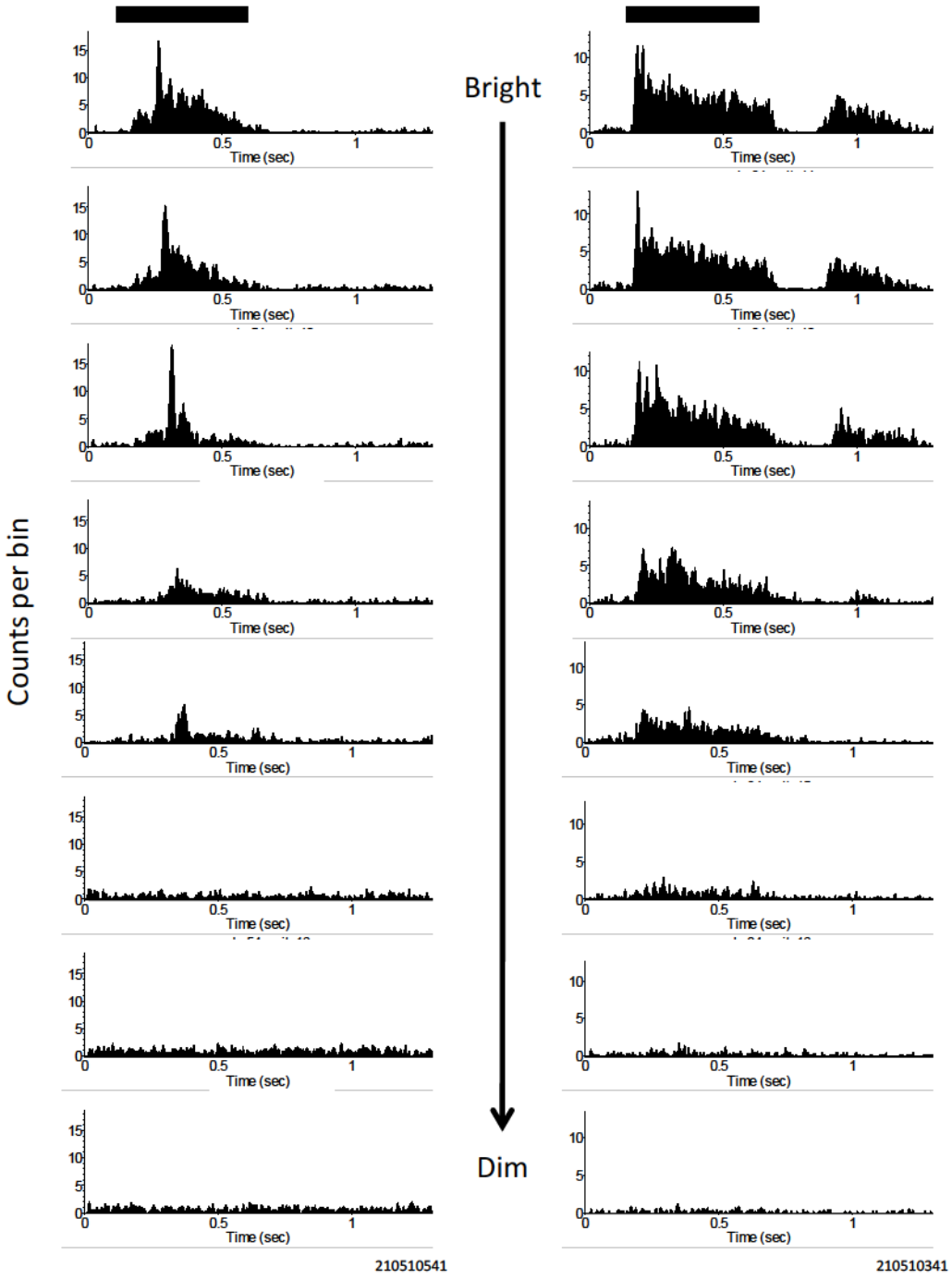

Figure 15. Effect of various light intensities on RGC spiking activity of individual cells. Two series of PSTHs from two cells recorded simultaneously from the same retinal preparation, illustrating the effect various light intensities on RGC spiking activity.

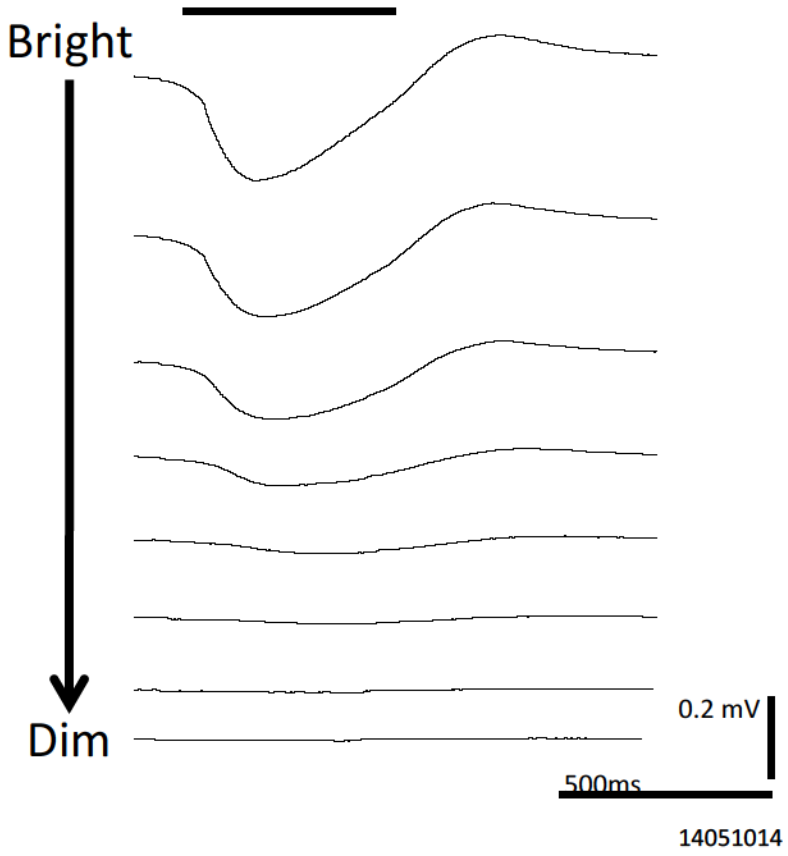

Figure 16. Effect of various light intensities on the ERG. Illustration of the average ERG collected from one MEA channel of a single retinal preparation as the light intensity was increasingly reduced.

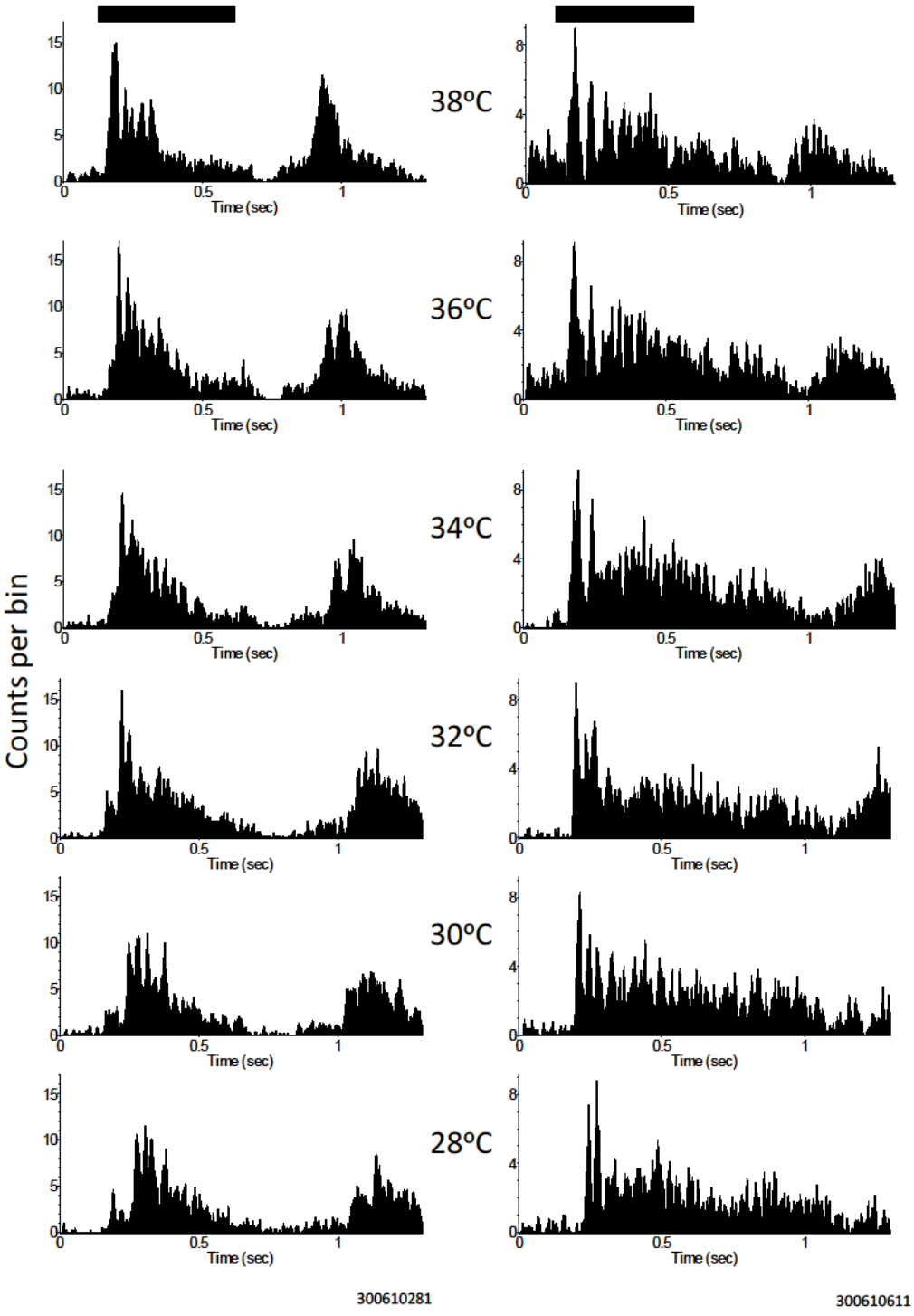

Figure 17. Effect of temperature on RGC spiking activity of individual cells.Two series of PSTHs from two cells recorded simultaneously from the same retinal preparation, illustrating the effect changing the MEA heating plate temperature on RGC spiking activity.

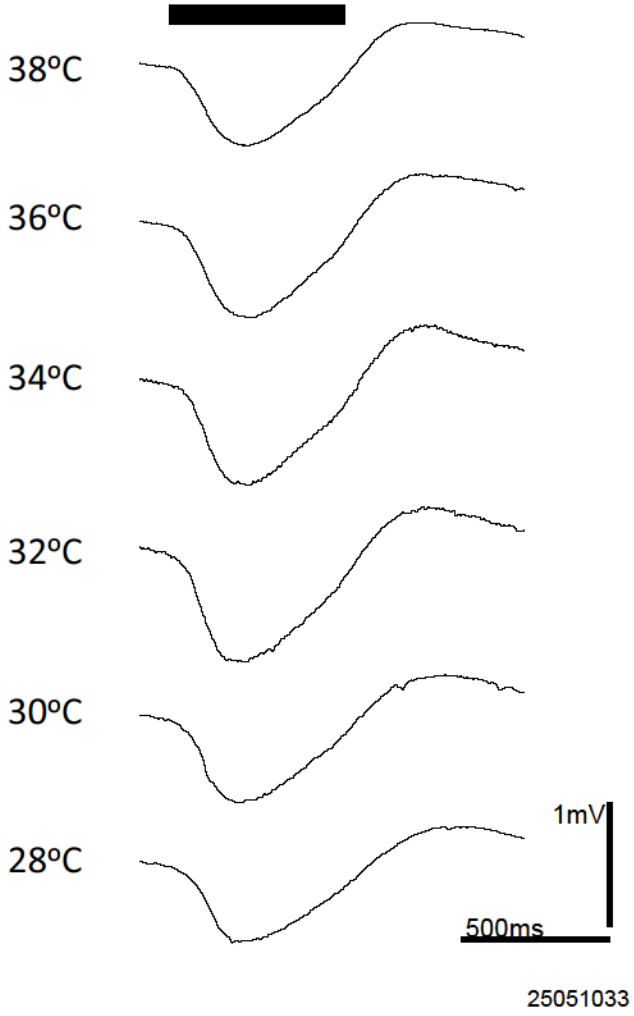

Figure 18. Effect of various heating plate temperatures on the average ERG collected from one MEA channel from a single retinal preparation.

The results in figure 19 indicate that the ON response was not significantly affected regardless of isoflurane exposure time; however, the OFF response was significantly affected for each trial. The effect of exposure to 1 MAC of isoflurane for varying time periods is illustrated in figure 22 by two representative example PSTHs from a single retinal preparation. The clinical dose (1 MAC) of anesthesia also had an impact on the ERG as shown in figure 23 and figure 21 I.c. when it was initially delivered to the retina; however, exposure to isoflurane for longer periods of time did not significantly impact the ERG.

The second portion of the experiment involved delivering varying concentrations of isoflurane to the retina (n=8) (figures 20 & 21). As seen in figure 20, one group comparisons reveal that at subclinical concentrations (<1MAC) isoflurane induced a non-significant reduction in the ON-associated RGC spiking activity and a significant reduction in the OFF-associated spiking activity. At clinical concentrations (1-2MAC) and greater (3-5MAC and >5MAC), ANOVA and sample t-tests demonstrate that both the ON (p=0.002) and OFF (p=0.008) spiking activity were reduced in a dose-dependent fashion (figure 20). Paired t-tests indicate that there was a significant difference comparing the ON and OFF components at subclinical concentrations only (figure 20). The effect of varying concentrations of isoflurane on retinal output is exemplified in the representative PSTHs in figure 24; individual cells in the same preparation may have different sensitivities to the same concentrations of isoflurane. There was no significant change in the percentage of tonic versus phasic cells despite being exposed to varying concentrations of isoflurane; however, the percentage of OFF cells did change significantly with increasing doses of isoflurane (p=0.030) (figure 21 II.b.).

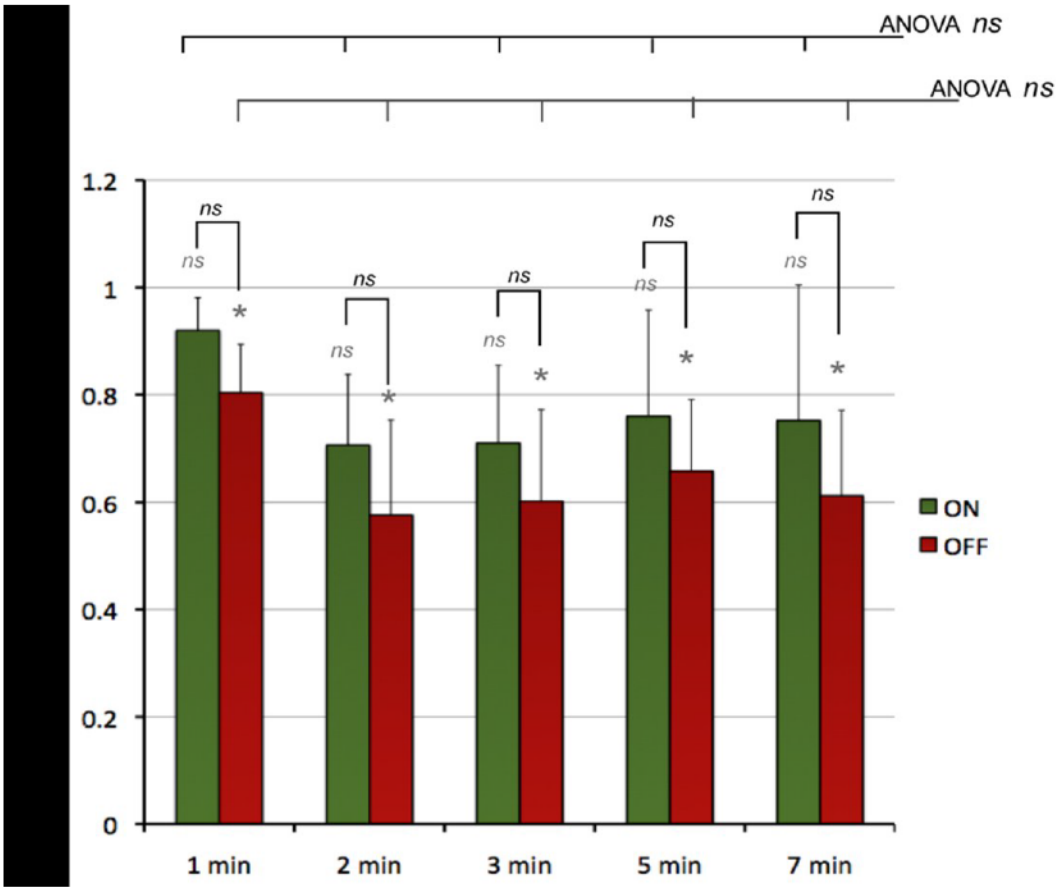

Figure 19. Effect of exposing the retina to 1MAC isoflurane solution for varying periods of time on the retinal ganglion cell spiking activity. One-group comparison (asterisk), paired comparison (ON-OFF) and ANOVA (full effect) are illustrated. Data is normalized to the recovery of the previous drug trial.

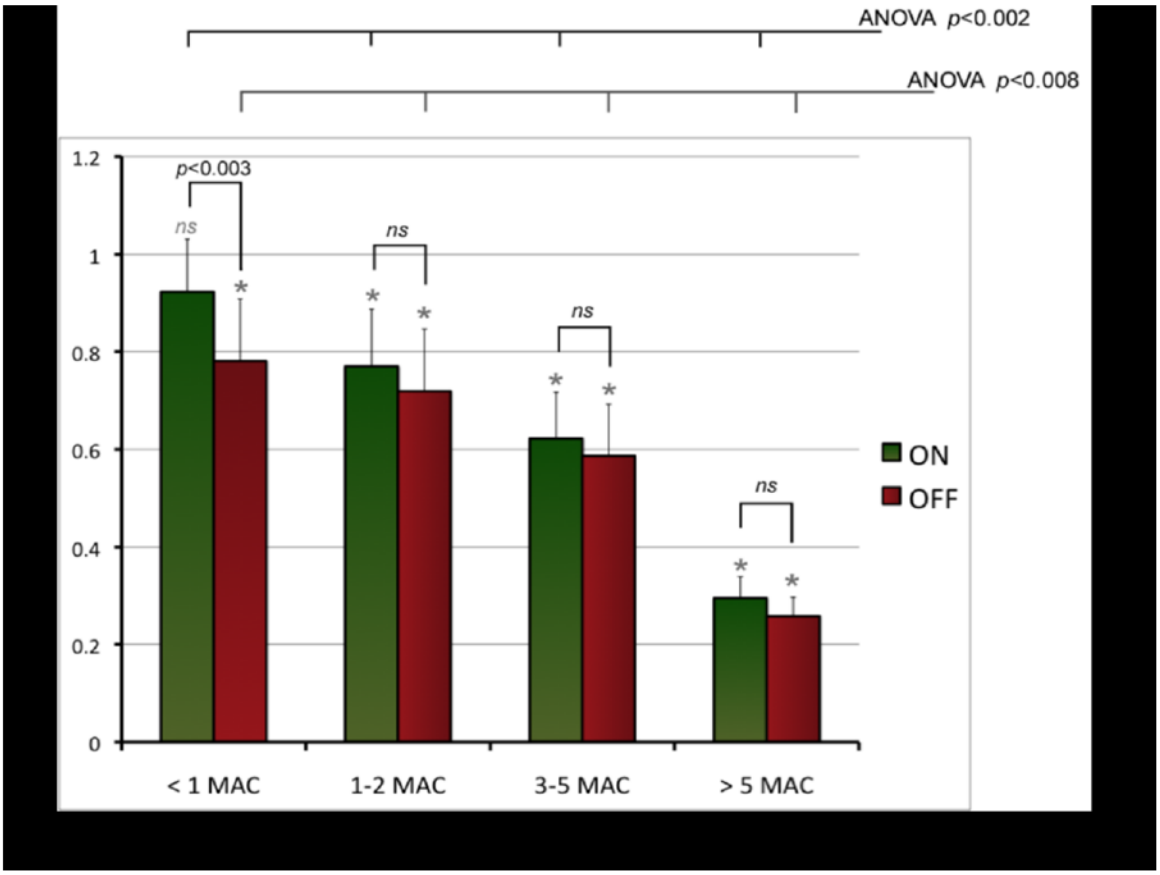

Figure 20. Effect of varying concentrations of isoflurane on retinal ganglion cell spiking activity. One-group comparison (asterisk), paired comparison (ON-OFF) and ANOVA (full effect) are illustrated. Data is normalized to the recovery of the previous drug trial.

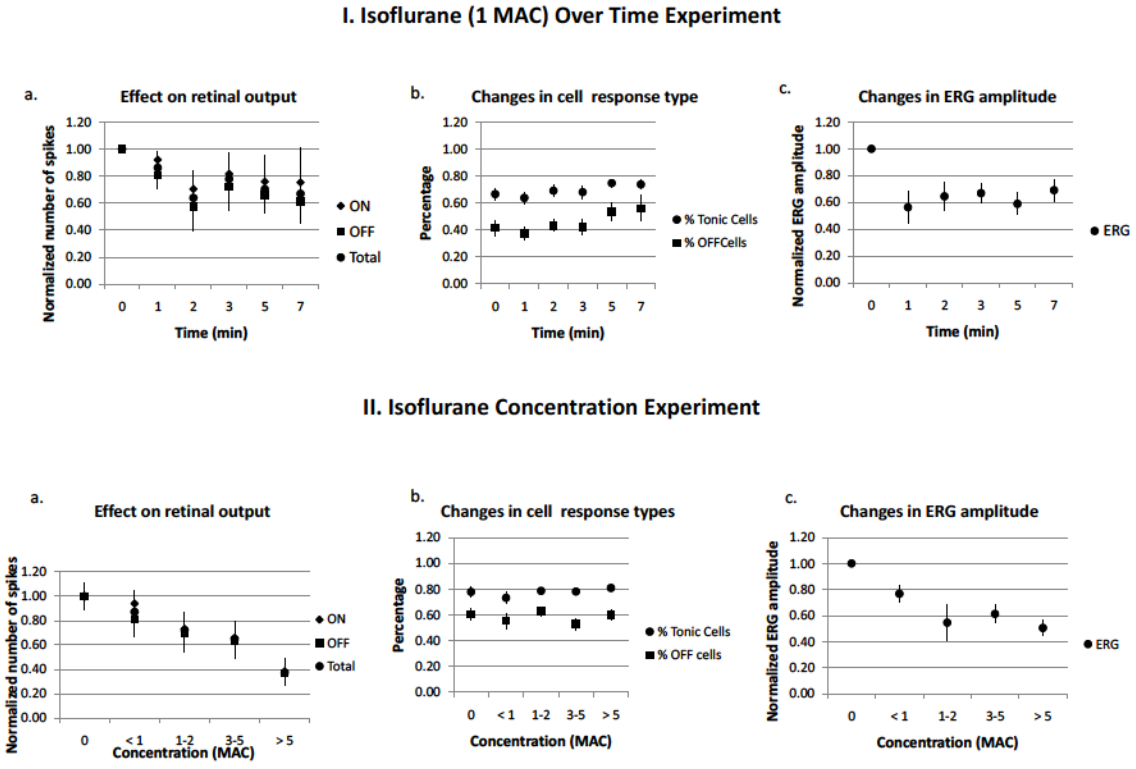

Figure 21. Effect of exposure to 1MAC of isoflurane for varying periods of time (I) and variations in isoflurane concentration (II) on RGC spiking activity (a), ON versus OFF and phasic versus tonic cell response types (b) and ERG amplitude (c). Data is normalized to the recovery of the previous drug trial.

Parameters	Isoflurane (1MAC) Over Time (n=5)	Isoflurane Concentration Experiment (n=8)
Effect on Total Retinal Output		
Spontaneous Activity	p= 0.810	**p= 0.030**
ON response	p= 0.930	**p= 0.002**
OFF response	p= 0.840	**p= 0.010**
Total Response	p= 0.850	**p= 0.005**
Type of Cell Response		
% Tonic	p= 0.290	p= 0.115
% OFF	p= 0.280	**p= 0.030**
ERG		
Amplitude	p= 0.840	**p= 0.000**

Table 2. Statistical ANOVA table for isoflurane experiments. ***p*<0.05**

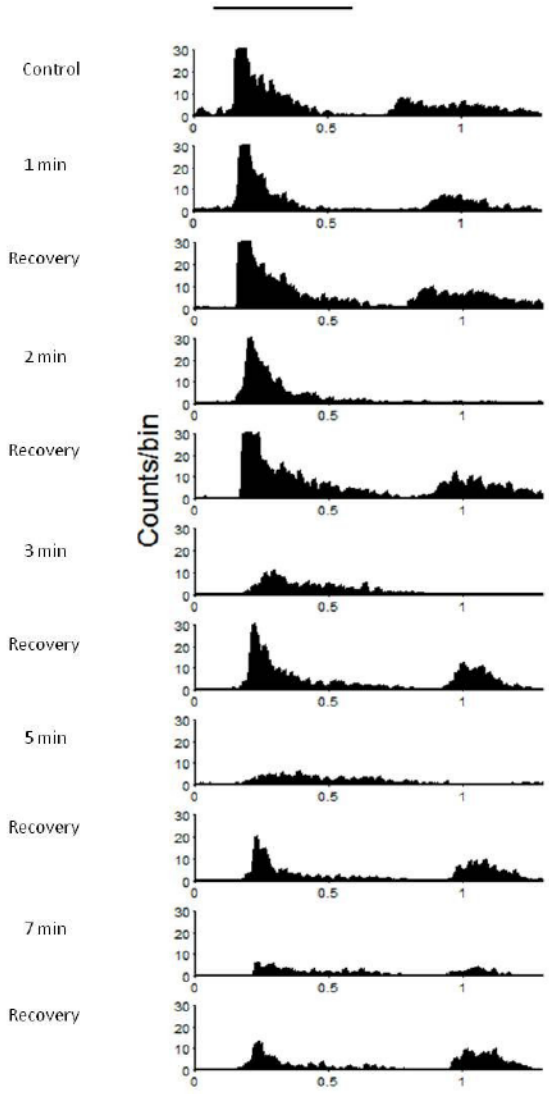

Figure 22. Effect of exposure time to1 MAC of isoflurane on RGC spiking activity of an individual cell. PSTHs from another retinal preparation illustrating effect of exposing the retina to isoflurane (1 MAC) for varying periods of time on RGC spiking activity.

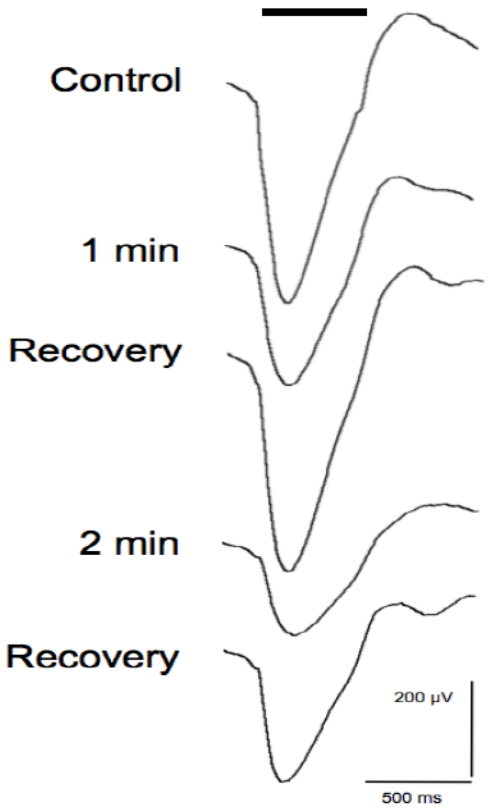

Figure 23. Effect of various exposure times of 1 MAC of isoflurane on the ERG. ERGs from one channel of the MEA demonstrating the ERG waveform under control conditions, during exposure of 1 MAC of isoflurane for 1 and 2 minutes and recoveries.

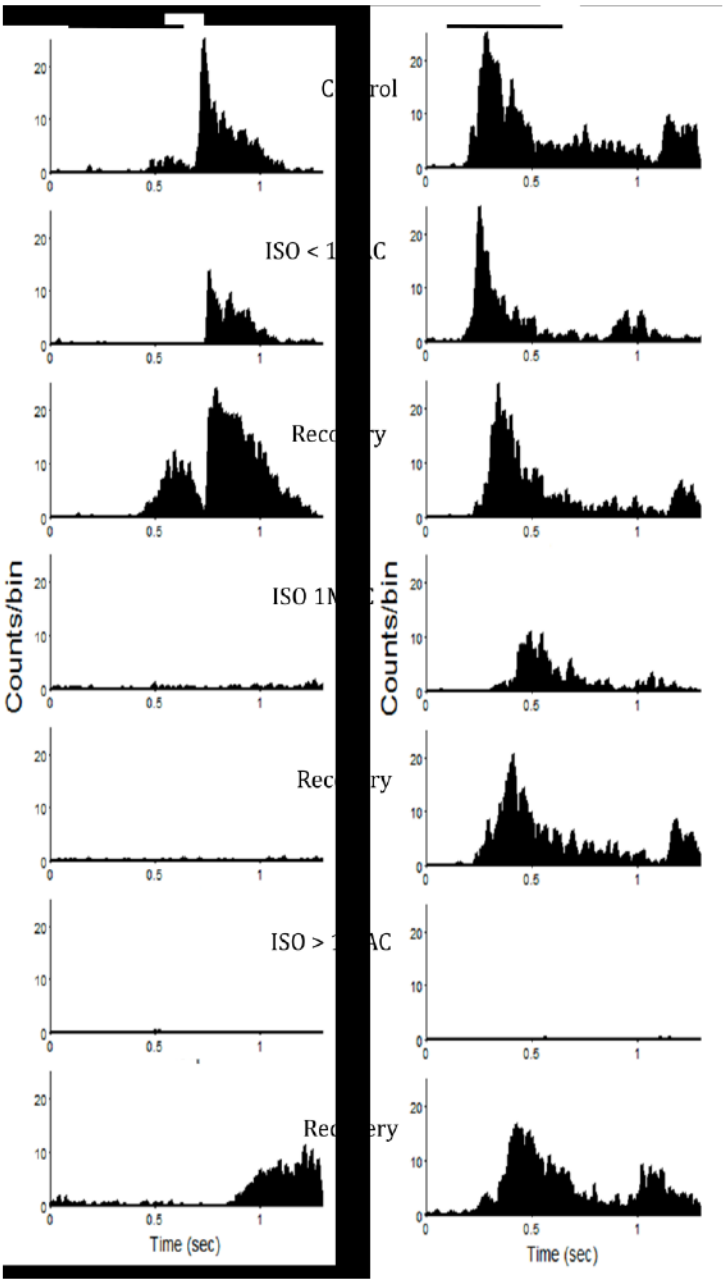

Figure 24. Effect of various concentrations of isoflurane on individual cells. Two series of PSTHs from two cells recorded simultaneously from the same retinal preparation, illustrating the dose-dependent effect of isoflurane.

Lastly, it is clearly shown in figure 21 II.c. that the amplitude of the ERG was significantly reduced as the concentration of isoflurane was raised (p=0.000).

3.4 Propofol Experiments

Varying concentrations (5µg/ml-1000µg/ml) of propofol were introduced to the retina by means of the MEA perfusion system (n=5). Normalized RGC spike counts demonstrate that at subclinical (5µg/ml) concentrations there was an increase of RGC spiking activity (figure 24). At clinical (10µg/ml), 5 times clinical, and 10 times clinical concentrations there was no significant reduction in RGC spiking activity. It was not until a very high concentration of propofol (1000µg/ml) was introduced to the retina that a significant reduction of spiking activity was observed. This point is further illustrated in figure 26 a. Although ANOVA analysis does reveal a significant change in the retinal output (spontaneous activity (p=0.008), ON (p=0.000) and OFF (p=0.000) responsive cells and total RGC output (p=0.000)), post-hoc analysis and individual sample t-test indicates that this statistical significance is driven by the substantial decrease of retinal output at 100 times the clinical concentration as well as by the excitation of RGC activity at subclinical concentration. Figure 27 shows two representative series of PSTH recorded simultaneously from the same retinal preparation with different sensitivities to the propofol drug. In these examples, no significant decrease in spike counts is observed until very high concentrations of propofol were introduced. Secondly, there is no significant impact observed on the percentage of phasic versus tonic cells or percentage of ON versus OFF cells as the concentration of propofol was increased (figure 26 b.). The average ERG amplitude was not significantly reduced with the introduction of varying concentrations of propofol (figure 26 c.) which is further exemplified in figure 28.

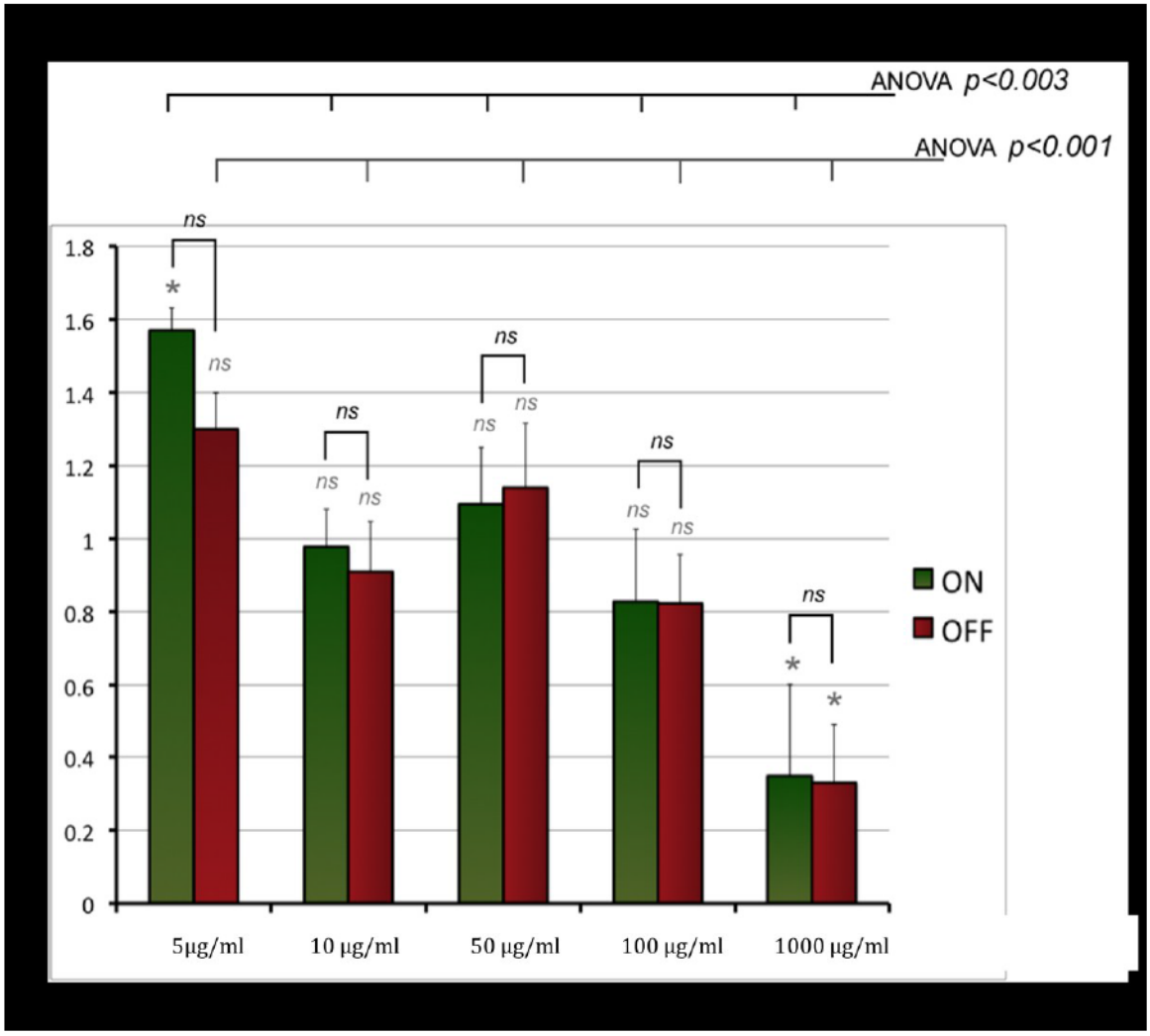

Figure 25. Effect of varying concentrations of propofol on RGC spiking activity. One-group comparison (asterisk), paired comparison (ON-OFF) and ANOVA (full effect) are illustrated. Data is normalized to the recovery of the previous drug trial.

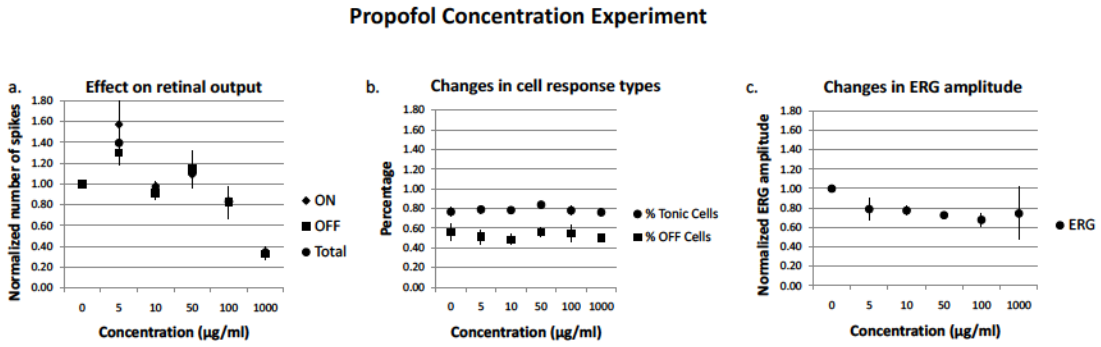

Figure 26. Effect variations in propofol concentration on RGC spiking activity (a), ON versus OFF and phasic versus tonic cell response types (b) and ERG amplitude (c). Data is normalized to the recovery of the previous drug trial.

Parameters	Propofol Concentration Experiment (n=5)
Effect on Total Retinal Output	
Spontaneous Activity	***p*= 0.008**
ON response	***p*= 0.000**
OFF response	***p*= 0.000**
Total Response	***p*= 0.000**
Type of Cell Response	
% Tonic	*p*= 0.720
% OFF	*p*= 0.910
ERG	
Amplitude	*p*= 0.570

Table 3. Statistical ANOVA table for propofol experiments. ***p*<0.05**

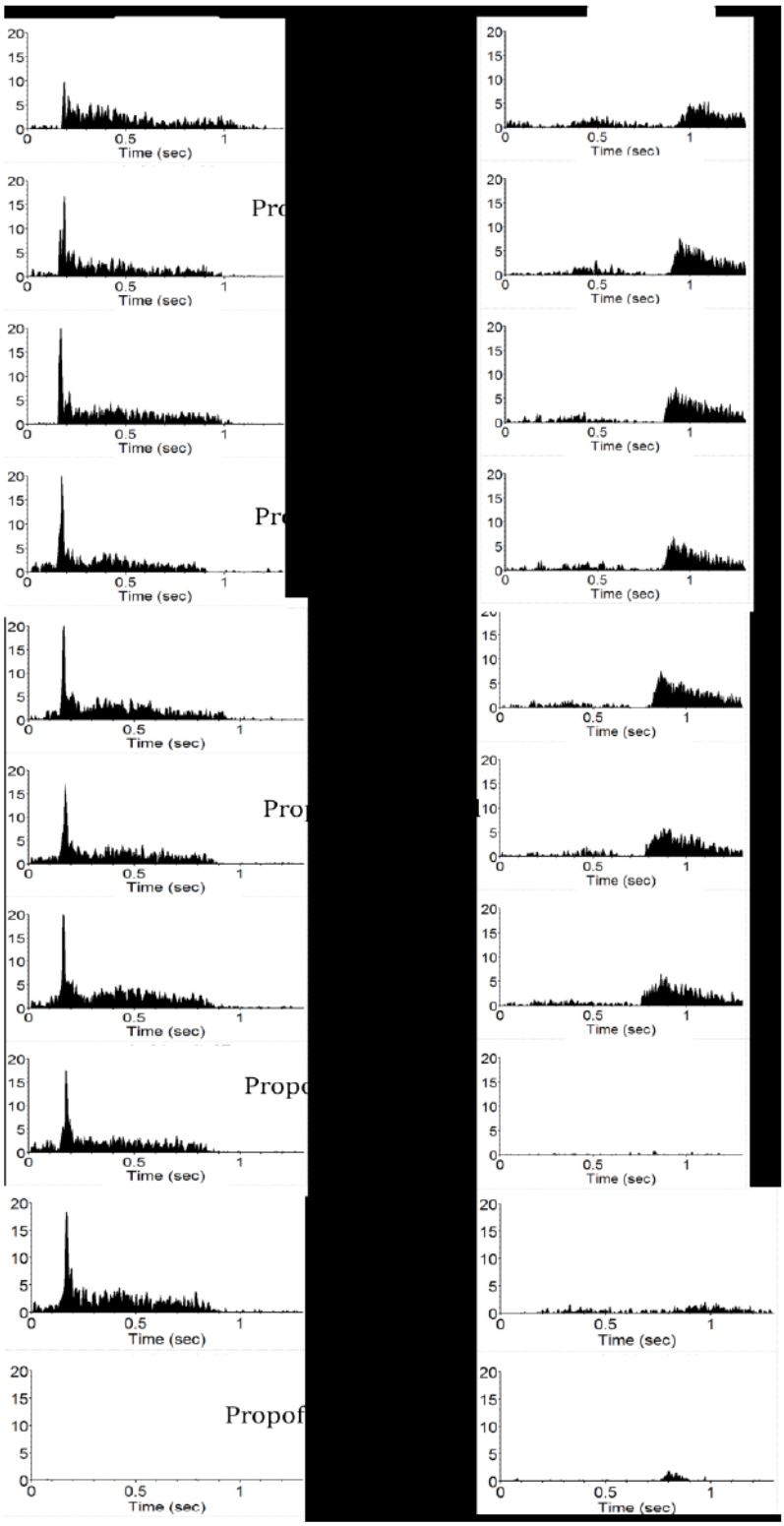

Figure 27. Effect of various concentrations of propofol on individual cells. Two series of PSTHs from two cells recorded simultaneously from the same retinal preparation, illustrating the effect of various concentrations of propofol on RGC activity.

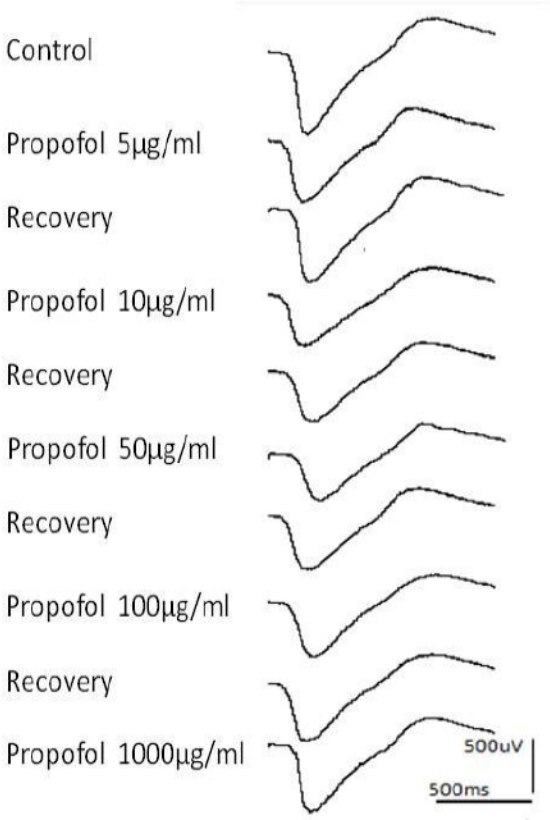

Figure 28. The effect of propofol on the average ERG from a single MEA channel from one retinal preparation.

All data analysis pertaining to this study has, up to now, been examined by analyzing the averages of retinal output in terms of quantification of number of spikes generated by the RGCs. Another form of analysis that could be performed would be to look at changes in the quality of the output of individual cells. Inter-stimulus interval (ISI) correlograms focus on qualitative changes occurring within individual cells rather than quantitative changes. By examining the intervals between spikes, it can be determined if there are changes in the RGC action potential firing patterns (i.e. the quality of the signal) being sent to the brain. This is referred to as neuronal entropy (Dorval et al., 2008). Figure 29 is a quantitative illustration of the variety of firing pattern in control conditions and under the influence of isoflurane anesthesia. Individual graphs are plots of the interval between I^{th} pair of spikes vs the I^{th} + 1 pair (or I^{th} interval and I^{th}+1 interval). Color refers to the relative frequency of occurrence of each pair of interval, in a 1ms bin width. One can appreciate that, in control condition, most cells tend to have a wide variety in their spiking intervals, thus referring to a larger entropy and higher capacity to transmit the information, according to communication theories. This is represented by a larger and more irregular area being plotted on the ISI graph. Under isoflurane, not only are fewer spikes generated (PSTH) but those spikes tend to be spiking more regularly resulting in lower entropy with a lower capacity to transmit complex information. This is represented by a smaller and more regular area plotted on the ISI graph. We have not performed a full quantification of this measure of entropy but the data readily opens that type of analysis. We also provide a representative example of what is happening in many cells under the influence of propofol (figure 30). Here the introduction of subclinical concentration of propofol increases the variety of intervals, thus enhancing the message

quality. The effect is reversible (recovery) and the use of larger concentration of propofol (50 μM) does not appear to change the cell output, either quantitatively (PSTH) or qualitatively (ISI). These two figures provide examples of potential ways to re-interpret the data generated for this thesis. Obviously, more analyses are needed before reaching any valuable conclusions.

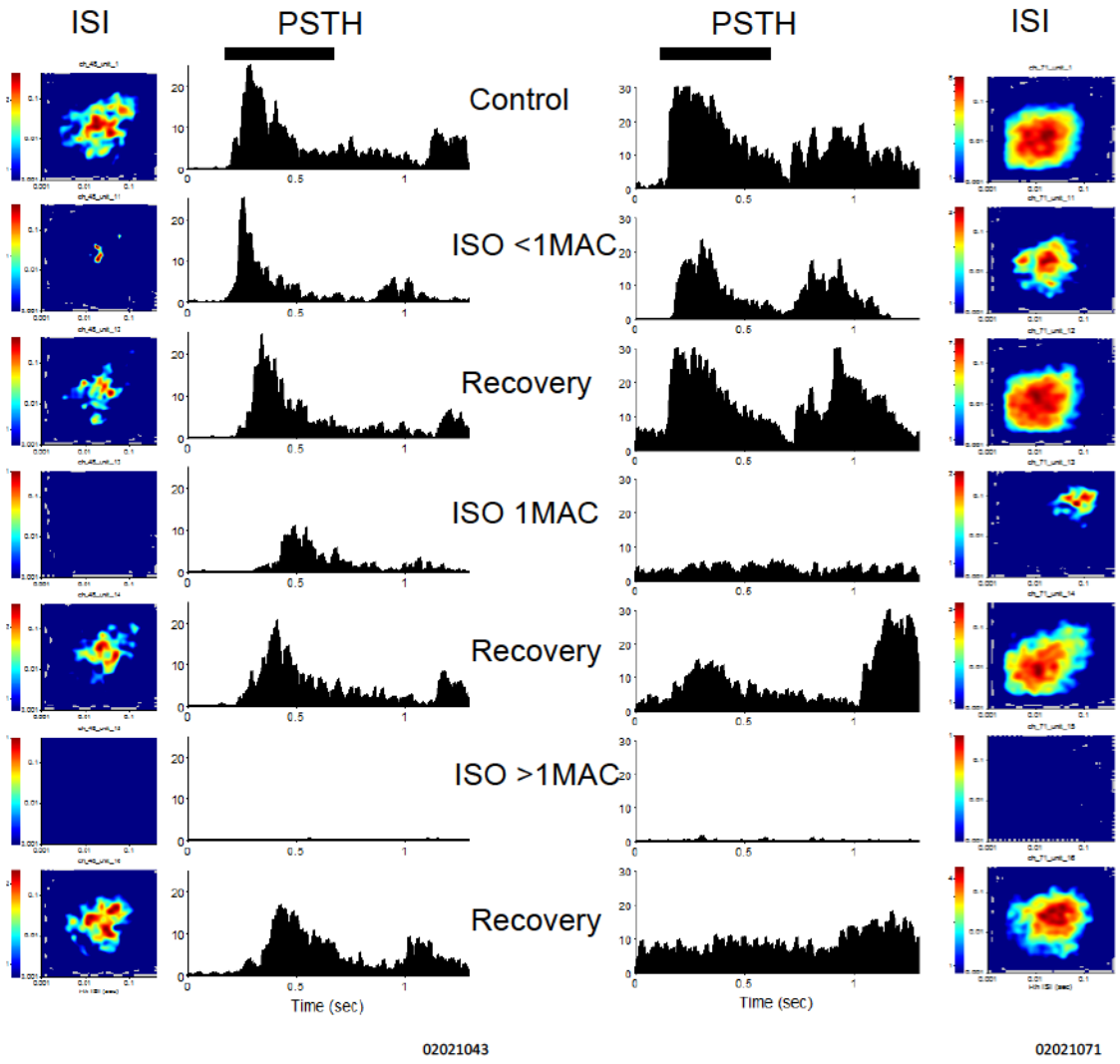

Figure 29. PSTH and inter-spike interval (ISI) graphs of a representative retinal cell exposed to varying concentrations of isoflurane. For the ISI, the difference between 2 spikes, s1 and s2, is on the x axis plotted with respect to the next interval s2-s3 on the y axis. Colors refer to the frequency of observation of such pairs.

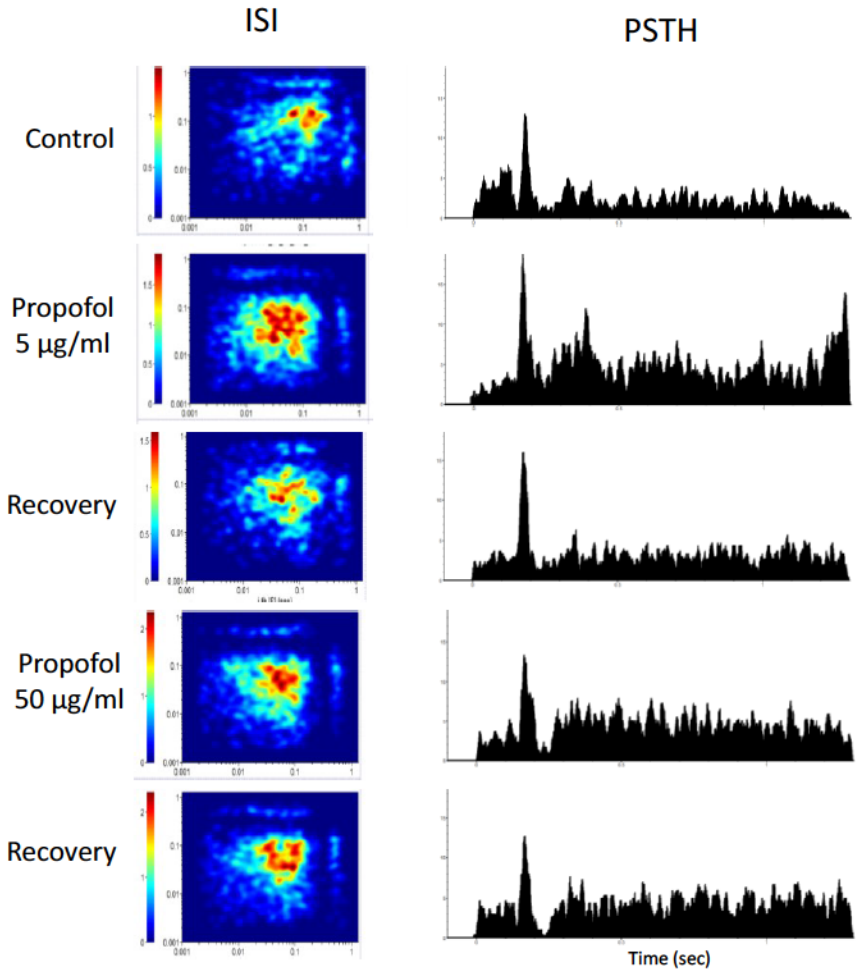

Figure 30. PSTH and inter-spike interval (ISI) graphs of a representative retinal cell exposed to varying concentrations of propofol. For the ISI, the difference between 2 spikes, s1 and s2, is on the x axis plotted with respect to the next interval s2-s3 on the y axis. Colors refer to the frequency of observation of such pairs.

CHAPTER 4: DISCUSSION

4.1 Technical Elements

4.11 On the Animal Model

The *in vivo* photopic ERG recordings performed in this study confirmed findings by Racine et al. (2005) that there are similarities between the photopic ERGs of humans and guinea pigs. The behavior of the OPs and long-duration stimuli ERGs are comparable in both guinea pigs and humans making the guinea pig a more appropriate animal model for the study of ON and OFF retinal system interactions than the rat or mouse. However, some differences do exist between the human and the guinea pig ERG signals. The most noticeable difference being the large contribution of negative components in the guinea pig ERG. Also, the OFF components identified in this study are of longer implicit time in the guinea pig, yielding a different interaction with the ON OPs responses than in human ERGs.

Furthermore, recent studies have demonstrated that the Nile grass rat may also be a superior animal model to the rat or mouse to represent human photopic ERGs. The photopic ERG waveform of the Nile grass rat exhibits a "photopic hill effect" similar to humans as light intensities are increased. They also demonstrate a positive OFF response to a long duration light stimulus as seen in guinea pigs and humans but not in rats or mice (Gilmour, et al., 2008).

The fact that guinea pigs, primates and the Nile rat share a similar photopic ERG to humans could possibly be due to the fact that they are all diurnal animals with cone rich retinas. Even though only 5% of human photoreceptors are cones, practically all photoreceptors in the foveal region are cones and it is from this region that the highest

visual acuity is derived (Osterberg, 1935). Guinea pig retinas contain 8-17% cone photoreceptors (Racine et al., 2008), while the Nile rat contains approximately 35% cone photoreceptors (Gaillard, et al., 2008). The retinas of both the rat and mouse contain mainly rod photoreceptors and very few cones because they are nocturnal animals (Solovei, et al., 2009).

4.12 On the Model Relevance

Figure 11 illustrates an increased latency of the OFF component over varying periods of exposure to isoflurane; however, there is no significant decrease in amplitude of this wave. The guinea pig photopic ERG appears much less affected under the influence of isoflurane than the human photopic ERG (figure 2). This may be due to a species variations or technical differences in the delivery of isoflurane to the guinea pig. For instance, isoflurane is often combined with N_2O in the OR and premedication (fentanyl I.V.) are given, as was the case with the Tremblay & Parkinson (2003) study. The combination of isoflurane and N_2O was found to depress the amplitude and increase the latency of the visual evoked potential (VEP), somatosensory evoked potential (SEP) and auditory brainstem response (ABR) in baboons. (Sloan, Sloan, & Rogers, 2010). It was found that isoflurane and N_2O had a synergistic effect (i.e. the effect is more than expected from the sum of individual effects) on these evoked potentials. The synergistic effect of isoflurane and N_2O in combination may explain why there was a much more significant impact on the amplitude of the b-wave and delay in implicit time in the human photopic ERG as oppose to the guinea pig ERG under the influence of isoflurane alone.

4.13 On Technical Considerations

The average number of cells recorded from a guinea pig retinal preparation in this study was 70.8 ± 16.4. Although reports of average cell count from a single retinal preparation on the MEA are rare, one study that recorded from mouse retinal preparation on the same type of MEA that was used in this study indicated that the average number of cells recorded from each retinal preparation was 46.7±4.4 (Ryu et al., 2009). In this study, a proportion of 52.4% ±14.3 of cells responded preferentially to the offset of the stimulus. A study using rabbit retinal preparations on the MEA observed 35.0±4.4% of ganglion cells responding to light onset, 30.4±1.9% responding to light offset and 34.6±5.3% responding to both ON and OFF stimuli (Jin, Ye, Lee, & Goo, 2005). Additionally, extracellular recordings in cat RGCs showed 49.1% to have OFF receptive fields; whereas, 50.9% had ON receptive fields (Tootle, 1993). The proportion of ON and OFF responding cells reported in these reports are similar to what is found in this study; however, it is important to note that in this study, we are simply quantifying cells that respond to the onset and offset of the light stimulus and not the receptive field properties of individual cells.

RGC action potentials from the guinea pig retina are seen immediately after the retinal slice is placed on the MEA and this study reveals that the total retinal output remains stable for at least a 2.5 hour period (figure 12 I.a.). On the contrary, while the RGC spiking activity remained stable, the ERG amplitude declined by a significant amount over time (figure 10 I.c.). Several experiments conducted throughout this study have lasted 4.5 to 5 hours. In most cases, the RGC spiking activity remained relatively stable and continued to be light responsive at the end of the experiment. The ERGs

continued to be present as well, despite a decline in amplitude. One report details that a rat retinal preparation must be placed on the MEA and perfused for an hour before spiking activity is detected and that the retina is only viable for approximately 1.5 hours (Hartwick, Moose, & Doerning, 2010). Perhaps the reason the guinea pig retinal output is more resistant to the effects of time as compared to the rat retina is related to the fact that the guinea pig retina is avascular. The avascular nature of the guinea pig retina may allow for a lower metabolic demand and stronger tolerance to changes in oxygen concentration, which could contribute its ability to survive longer *ex vivo* than the rat retina.

Furthermore, as demonstrated in figure 10 II.a., the RGC spiking activity reaches saturation at the brightest light intensities that were presented to the retina. Interestingly, the ERG amplitude reaches its semi-saturation constant before the retinal output (figure 10 II.c.). This finding provides a possible explanation for the difference in decline over time between ERG and RGC activity. The fact that ERG semi-saturation constant is much higher than the RGC semi-saturation constant means that, at high intensities, the RGC activity saturates (i.e. is not responsive to changes in illumination), while the ERG activity is still responsive (i.e. the ERG amplitude still changes with increasing intensities). As the stimulus used in the baseline over time study was set at the highest intensity, it would mean that the RGC variations are less sensitive to photon-capture processing deterioration over time. Another finding in this experiment is that, when the illumination is decreased, the cell response types shift in the direction of a greater percentage of OFF responding cells as oppose to those responding to an ON stimulus.

As demonstrated in figure 10 III.c., temperature reductions induced an overall reduction of the ERG amplitude. This effect has also been described in both *in vivo* and *in*

vitro studies of numerous species. *In vitro* retinal cooling by lowering the temperature of the bathing media in the goldfish and rat retinas showed a progressive reduction in amplitude and increased implicit time of all ERG components (Dawson, Hope, & Bernstein, 1971; Winkler, 1972). *In vivo* experiments carried out in rabbits that involved cooling the retina by circulating a cooling solution through plastic tubing coiled around the eye demonstrated a reduction in amplitude and increase in peak times of all ERG components but to a lesser extent than *in vitro* studies (Lachapelle et al., 1996). Studies that lowered the core body temperature of mice also found a significant reduction in both the a- and b-waves of the ERG (Adachi-Usami & Mizota, 2002; Kong & Gouras, 2003). In out *ex vivo* model, despite the reduction in ERG amplitude, the total RGC spiking activity remained relatively stable. This discrepancy in the sensitivity of the ERG and total retinal output due to temperature may be again explained by the relative insensitivity of the RGCs to the photon-capture processing as is seen in the light intensity experiment.

4.2 Effect of Anesthetic Agents on the Retina

4.21 Effect of Isoflurane and Propofol on Retinal Output

It is known that both isoflurane and propofol impact cortical activity through various molecular mechanisms. Recent *in vivo* and *in vitro* studies using various animal models have also investigated the effect of these anesthetic agents on retinal activity.

Lalonde et al. (2006) have demonstrated that isoflurane impacts the pattern and multi-focal ERG signals in a similar way to tetrodotoxin (TTX) and optic nerve axotomy in a pig model. Their results suggest reduced RGC activity under isoflurane anesthetic conditions, which coincides with the diminished retinal output observed under the influence of isoflurane in this study. In contrast to this finding, another group has

observed an increase in amplitude of all multi-focal ERG waveform components in a perfused porcine eye *in vitro* under the influence of isoflurane anesthesia (Ng, Chan, To, & Yap, 2008).

Others have reported modifications to the ERG waveform in *in vivo* animal models as a result of isoflurane anesthesia. A reduction in the b-wave amplitude and increase in implicit time were shown in the photopic ERGs of mice under isoflurane anesthesia as opposed to ketamine anesthesia (Woodward, et al., 2007). Jeong et al. (2009) compared the effect of three anesthetic combinations (thiopental-isoflurane (TI), medetomine-ketamine (MK), and xylazine-ketamine (XK)) on the ERGs of miniature schnauzer dogs. They determined that under photopic conditions, there was no significant difference in the amplitude or implicit time of the a-wave among the three anesthetic protocols, however, they found a significant reduction in the amplitude and increase in implicit time of the b-wave under TI conditions as compared to MK and XK. Both of these studies are in accordance with the Tremblay & Parkinson (2003) study. Another group compared the effect of tiletamine-zolazepam sedative and isoflurane general anesthesia on the photopic ERG. Their findings revealed that isoflurane induced a greater reduction of both the a- and b-wave amplitude than the sedative agent (Lin et al., 2009). These findings are in accordance with the results of this study as both ON and OFF responsive RGC activity were diminished with exposure to the clinical and greater than clinical doses of isoflurane.

Propofol has also been shown in the literature to influence retinal activity. This anesthetic agent has been shown to increase the amplitude of the b-wave with increasing doses of propofol in the scotopic ERG of a dog (Kommonen, Hyvatti, & Dawson, 2007).

Another group compared the effect of propofol and thiopentone on the scotopic pig ERG. They found that propofol had no significant effect on the amplitude of the ERG waves and concluded that propofol better preserved photoreceptor sensitivity because it demonstrated a shorter implicit time and steeper a-wave than thiopentone (Tanskanen, Kylma, Kommonen, & Karhunen, 1996). The multi-focal ERG study of the perfused porcine eye by Ng et al. (2008) concluded that propofol did not significantly impact the amplitude of the waveform but did significantly increase the implicit times of each waveform component.

The effect of anesthetics has also been more extensively studied on the visual evoked potential (VEP) which is a measure of the electro- encephalographic activity recorded at the scalp after the presentation of a visual stimulus. It provides diagnostic information about the functional integrity of the visual system (Odom, et al., 2004). A group tested the VEP and pattern ERG acuity in rhesus monkeys anesthetized with propofol. They determined that even large concentrations of propofol (8 times clinical dosage) did not degrade the VEP or pattern ERG acuity and concluded that propofol shows only minimal effects on the transmission of high contrast spatial-frequency from the retina to the cortex (Ver Hoeve, Danilov, Kim, & Spear, 1999). This finding provides further support for this present study as it indicates that propofol does not have a significant impact on the retina because the information being carried by the ganglion cells to the cortex is not impacted. In contrast, Nakagawa et. al compared the effect of sevoflurane, another halogenated anesthetic, with propofol on the VEP, SEP and auditory brain stem response (ABR). They discovered that sevoflurane significantly reduced the amplitude of the VEP and SEP but produced less marked changes to the ABR. Propofol

decreased the VEP significantly but no significant changes to the SEP and ABR were observed (Nakagawa, 2006). These studies provide contradictory evidence of the effect of propofol on cortical processing and requires further investigation; however, the results of this study favor the idea that propofol has a minor impact on neuronal processing.

4.22 Proposed Mechanism of Action of Isoflurane and Propofol on the Retina

Due to the multipotent nature of general anesthetics, it is difficult to propose the molecular mechanisms by which they exert their effects on the retina. At clinical concentrations, isoflurane is known to interact with various ion channels that are present in the retina such as ACh, $GABA_A$, AMPA and NMDA glutamate receptors and voltage-gated sodium channels (Campagna et al., 2003). Therefore, it is possible that isoflurane interferes with the synaptic circuits presynaptic to RGCs to prevent RGC action potentials, as we have demonstrated that the ERG amplitude was reduced under the influence of isoflurane. Isoflurane may also influence RGC action potentials directly by interacting with voltage-gated sodium channels, which would also contribute to the prevention of RGC firing. This idea is supported by a study that was carried out in this laboratory that investigated the effect of isoflurane on field potentials recorded directly from the optic nerve. The unpublished data revealed that isoflurane did completely attenuate the optic nerve field potential.

Propofol is known to potentiate inhibitory $GABA_A$ receptors (Solt & Forman, 2007). $GABA_A$ receptors influence signaling from amacrine cells to bipolar cells and ganglion cells (Kolb et al., 1995); therefore, it is surprising that no significant changes retinal output were recorded under the influence of propofol. Although, it does support the idea that no significant changes were seen in the ERG signal under the influence of

propofol because amacrine and ganglion cell activity do not provide a strong contribution to the ERG signal.

An investigation examining the effect of isoflurane and nitrous oxide in combination versus propofol on the motor evoked potentials (MEP) determined that propofol is a more appropriate anesthetic than isoflurane and nitrous oxide to record muscular activity. Another study that investigated the differential effects of isoflurane and nitrous oxide on the auditory evoked potential (AEP) and the somatosensory evoked potential (SEP) determined that isoflurane had a more depressive effect on the AEP; whereas, nitrous oxide had a more depressive effect on the SEP. One study involving the measurement of auditory evoked response under propofol anesthesia showed no significant effect on brainstem-evoked response latencies and interpeak intervals; however, increasing latencies and reduction of wave amplitudes were observed in the cortical-evoked components (Thornton, et al., 1989). Another study used functional magnetic resonance imaging to monitor various brain structures during the transition from awake to unresponsive under propofol anesthesia. This study revealed a clear reduction in the functional connectivity between the putamen and many other cortical and sub-cortical structures, while the connectivity of the thalamus with these structures was maintained (Mhuircheartaigh et al., 2010). These studies exemplify that anesthetics can reduce activity of specific regions of the brain while not affecting others; therefore, it is possible that propofol may not have a strong influence on retinal activity while having an impact on subcortical/cortical one.

4.23 Limitations

One limitation associated with this study is the fact that the drug concentrations

used were not measured directly by the investigators of this study. All concentrations used were based on formulations found in the literature. Not all components of the MEA set-up were gas tight such as the plastic syringe in the syringe pump, plastic tubing and perfusion chamber; therefore, some isoflurane may have escaped due to its volatile nature. This means that the isoflurane concentrations used in this study could only be less than what is quoted in the literature, yet even at less than clinical concentrations, isoflurane produces an effect on retinal output. Also, the human drug concentrations were used in this study and not the equivalent concentrations for guinea pig models. Higher concentrations of the anesthetics may be needed in guinea pigs to produce similar anesthetic conditions as seen in humans; however, to our knowledge, comparative concentration data is not currently available in the literature.

A second limitation is the fact that the guinea pig photopic ERG occurring *ex vivo* on the MEA does not resemble that of the guinea pig *in vivo*. Pharmalogical dissociation of the ERG signal obtained on the MEA is needed to determine what retinal components are contributing to the *in vitro* ERG waveform.

This study is also limited by the fact that the experiments were performed *ex vivo* which does not take into account any metabolic or other secondary biological effects (i.e. cardiovascular effects, respiratory effects, etc) that may be present *in vivo*.

Lastly, only two anesthetics were tested in this investigation. Since anesthetics are often administered in combination in the OR it is necessary to investigate the effect of other anesthetics families on retinal output to determine the best anesthetic combination for diagnostic procedures involving the retina. This is important not only for clinical studies but also for animal studies as it has an impact on how data is interpreted.

4.24 Future Studies

The results of this study have the potential to generate several future projects involving anesthesia and MEA technology. This study examined the effect of anesthetics on RGC action potentials and ERGs generated by a single light intensity. Data collected from other light intensities during this project will be analyzed in the future to determine if the effects are similar when other intensities are used. Furthermore, this report only examined the effect isoflurane and propofol on the total number of RGC action potentials. The next step in this process is to investigate how these drugs affect the quality of the RGC signal. Studies using entropy mathematical approach could greatly benefit from this approach as the quality of the retinal message is as important as the quantity of information that is delivered to the brain. This may be done by quantitating the interspike intervals as shown in figure 27.

Further studies are also needed to investigate the guinea pig ERG waveform recorded using the MEA configuration. *In vivo* guinea pig ERGs clearly demonstrate a negative a-wave followed by a positive b-wave; however, this waveform could not be reproduced *ex vivo* on the MEA. A positive b-wave was recorded from a rat retina using the identical MEA configuration; therefore, the odd ERG produced by the guinea pig ERG is not due to the spacing or impedence of the electrodes, position of the reference electrode, etc. Further pharmacological studies are necessary to understand what retinal neurons are contributing to the negative ERG waveform produced by the guinea pig retina.

It is also necessary to record directly from various positions along the visual pathway to understand whether the reduced activity at the visual cortex under the

influence of isoflurane anesthesia is purely a result of the reduced RGC activity or a combination of the anesthetic effect both the visual cortex and RGC activity directly.

Lastly, this study shows that MEA technology can easily be implemented to study the effects of various pharmacological agents on retinal activity. This equipment could be used to investigate the effects of various anesthetics on the retina.

4.3 Conclusion

The retinal output, as measured by RGC activity, is selectively influenced by exposure to isoflurane. Even at subclinical doses, the OFF component appears more affected, as suggested by the clinical ERGs recorded under isoflurane in the operating room. In contrast, propofol appears to have very limited effects on ERG and RGC activity at clinical concentrations, which suggests that propofol is a more appropriate choice of anesthetic agent to use when evaluating the retinal activity in the OR.

Although further investigation is required to understand completely the interactions maintained by the neural generators of the guinea pig ERG, this newly developed and "standardized" animal model offers excellent potential for retinal research particularly when ON and OFF interactions are being studied. In addition, the MEA technology can easily be implemented to suit pharmacological and network retinal studies. This technique offers the advantage of comparing simultaneously photoreceptor and post-receptoral processing (in the form of ERG data) with the retinal output (in the form of retinal ganglion cell activity).

General anesthetics exercise their action through several mechanisms that impact neural processing in various ways in different neural structures. For the visual system, it

appears that anesthesia affects the retinal processing, and this should be considered in any animal studies, whether investigating the retina or the cortex physiology.

REFERENCES

Achar, S., & Kundu, S. (2002). Principles of office anesthesia: Part I. infiltrative anesthesia. *American Family Physician , 66* (1), 91-94.

Adachi-Usami, E., & Mizota, A. (2002). Effect of body temperature on the electroretinogram of mice. *Investigative Ophthalmology & Visual Science , 43* (12), 3754-3757.

Altman, J. (1962). Diurnal activity rhythm of rats with lesions. *The American Journal of Physiology , 202*, 1205-1207.

Andrew, D., Leslie, K., Sessler, D., & Bjorksten, A. (1997). The arterial blood propofol concentration preventing movement in 50% of healthy women after skin incision. *Anesthesia & Analgesia , 85*, 414-419.

Andrews, D., Leslie, K., Sessler, D., & Bjorksten, A. (1997). The arterial blood propofol concentration preventing movement in 50% of healthy women after skin incision. *Anesthesia & Analgesia , 85*, 414-419.

Bai, D., Pennefather, P., MacDonald, J., & Orser, B. (1999). The general anesthetic propofol slows deactivation and desensitization of GABA(A) receptors. *Journal of Neuroscience , 19*, 10635-10646.

Barash, P. G., Cullen, B. F., Stoelting, R. K., & Cahalan, M. (2009). *Clinical anesthesia* (6th edition ed.). Philadelphia: Lippincott Williams & Wilkins.

Baylor, D. (1987). Photoreceptor signals and vision. Proctor lecture. *Investigative Opthalmology and Visual Science , 28* (1), 34-49.

Bui, B., & Fortune, B. (2004). Ganglion cell contributions to the rat full-field electroretinogram. *The Journal of Physiology , 555*, 153-173.

Campagna, J., Miller, K., Phil, D., & Forman, S. (2003). Mechanisms of actions of inhaled anesthetics. *The New England Journal of Medicine , 348*, 2110-2124.

Chalupa, L., & Gunhan, E. (2004). Development of On and Off retinal pathways and retinogeniculate projections. *Progress in Retinal and Eye Research* , 31-51.

Dawson, W., Hope, G., & Bernstein, J. (1971). Goldfish retina structure and function in extended cold. *Experimental Neurology , 31*, 368-382.

Debrabant, F., Hache, J., Cantineau, D., & Scherpereel, P. (1984). Influence of low concentrations of halogenated anesthetics on the electroretinogram and visual evoked potentials in children. *Annales Françaises d'Anesthésie et de Réanimation , 3* (2), 99-104.

Dorval, A., Russ, G., Hashimoto, T., Xu, W., Grill, W., & Vitek, J. (2008). Deep brain stimulation reduces neuronal entropy in the MPTP-primate model of Parkinson's disease. *Journal of Neurophysiology , 100*, 2807–2818.

Eggenberger, T., Haworth, K., Mills, J., Page, S., Robinson, K., & Thakuria, F. (2001). *Clinical pharmacology made incredibly easy.* Pennsylvania: Springhouse Corporation.

Franks, N., & Lieb, W. (1996). Temperature dependence of potency of volatile general anesthetics: implications for in vitro experiments. *Anesthesiology , 84* (3), 716-720.

Gaillard, F., Bonfield, S., Gilmour, G., Mema, S., Martin, B., Smale, L., et al. (2008). Retinal anatomy and visual performance in a diurnal cone-rich laboratory rodent, the Nile grass rat (Arvicanthis niloticus). *The Journal of Comparative Neurology , 510*, 525-538.

Ghoneim, M., & Mewaldt, S. (1990). Benzodiazepines and human memory: A review. *Anesthesiology , 72*, 926-938.

Gilmour, G., Gaillard, F., Watson, J., Kuny, S., Mema, S., Bonfield, S., et al. (2008). The electroretinogram (ERG) of a diurnal con-rich laboratory rodent, the Nile grass rat (Arvicanthis niloticus). *Vision Research , 48*, 2723-2731.

Gjotterberg, M. (1986). Electrodes for electroretinography. *Archives of Ophthalmology , 104* (4), 569-570.

Gouras, P. (1970). Electroretinography: Some basic principles. *Investagative Ophthalmology , 9* (8), 557-569.

Grasshoff, C., Drexler, B., Rudolph, U., & Antkowiak, B. (2006). Anaesthetic drugs: Linking molecular actions to clinical effets. *Current Pharmaceutical Design , 12*, 3665-3679.

Hales, T., & Lambert, J. (1991). The actions of propofol on inhibitory amino acid receptors of bovine adrenomedullary chromaffin cells and rodent central neurones. *British Journal of Pharmacology , 104*, 619-628.

Hara, M., Kai, Y., & Ikemoto, Y. (1993). Propofol activates GABA(A) receptor-chloride ionophore complex in dissociated hippocampal pyramidal neurons of the rat. *Anesthesiology , 79*, 781-788.

Hartwick, A., Moose, H., & Doerning, C. (2010). Firing activity of intrinsically photosensitive retinal ganglion cells during prolonged light stimulation. *XIX Biennial Meeting of the International Society for Eye Research* (p. 327). Montreal: International Society for Eye Research.

Haverkamp, S., & Wassle, H. (2004). Characterization of an amacrine cell type of the mammalian retina immunoreactive for vesicular glutamate transporter 3. *The Journal of Comparative Neurology , 468*, 251–263.

Heckenlively, J., & Arden, G. (1991). *Principles and practice of clinical electrophysiology of vision* (1st Edition ed.). St Louis, MO: Mosby-Year Book, Inc.

Heckenlively, J., & Arden, G. (2006). *Principles and practice of clinical electrphysiology of vision* (2nd Edition ed.). Cambridge: MIT Press .

Jeong, M., Narfstrom, K., Park, S., Chae, J., & Seo, K. (2008). Comparison of the effects of three different combinations of general anesthetics on the electroretinogram of dogs. *Documenta Opthalmologica , 119*, 79-88.

Jin, G., Ye, J., Lee, T., & Goo, Y. (2005). Electrical stimulation of isolated rabbit retina. *Engineering in Medicine and Biology 27th Annual Conference*, (pp. 5967-5970). Shanghai.

Keller, C., Grimm, C., Wenzel, A., Hafezi, F., & Reme, C. (2001). Protective effect of halothane anesthesia on retinal light damage: Inhibition of metabolic rhodopsin regeneration. *Investigative Ophthalmology and Visual Science , 42* (2), 476-480.

Kitahata, L., & Saberski, L. (1992). Are barbiturates hyperalgesic? *Anesthesiology , 77* (6), 1148-1154.

Kolb, H. (2003). How the retina works. *American Scientist , 91*, 28-35.

Kolb, H., Fernandez, E., & Nelson, R. (1995). *Webvision: The organization of the retina and visual system.* Retrieved May 14, 2010, from National Center for Biotechnology Information: http://www.ncbi.nlm.nih.gov/bookshelf/br.fcgi?book=webvision

Kommonen, B., Hyvatti, E., & Dawson, W. (2007). Propofol modulates inner retina function in Beagles. *Veterinary Opthalmology , 10* (2), 76-80.

Kong, J., & Gouras, P. (2003). The effect of body temperature on the murine electroretinogram. *Documenta Ophthalmologica , 106* (3), 239-242.

Lachapelle, P., Benoit, J., & Guite, P. (1996). The effect of in vivo retinal cooling on the electroretinogram of the rabbit. *Vision Research , 36* (3), 339-344.

Lei. The ERG of guinea pig (Cavis porcellus): comparison with I-type monkey and E-type rat. (2003) Documenta ophthalmologica Advances in ophthalmology., 106 (3) pp. 243-9

Lerman, J., & Jorh, M. (2009). Inhalational anesthesia vs total intravenous anesthesia (TIVA) for pediatric anesthesia. *Pediatric Anesthesia , 19*, 521-534.

Lin, S., Shiu, W., Liu, P., Cheng, F., Lin, Y., & Wang, W. (2009). The effects of different anesthetic agents on short electroretinography protocol in dogs. *Internal Medicine , 71* (6), 763-768.
Lullman, H., Ziegler, A., Mohr, K., & Bieger, D. (2000). *Color Atlas of Pharmacology* (2nd Edition ed.). New York: Thieme Stuttgart.

Malviya, S., & Lerman, J. (1990). The blood/gas solubilities of sevoflurane, isoflurane, halothane, and serum constituent concentrations in neonates and adults. *Anesthesiology , 72*, 793-796.

Marc, R., Murry, R., & Basinger, S. (1995). Pattern recognition of amino acid signatures in retinal neurons. *The Journal of Neuroscience , 15* (7), 5106-5129.
Masland, R. (2001). The fundamental plan of the retina. *Nature Neuroscience , 4* (9), 877-886.

McDougall, S., Peters, J., LaBrant, L., Wang, X., Koop, D., & Andresen, M. (2008). Paired assessment of volatile anesthetic concentrations with synaptic actions recorded in vitro. *Plos ONE , 3* (10), e3372.

McKenzie, D., Franks, N., & Lieb, W. (1995). Actions of general anaesthetics on a neuronal nicotinic acetylcholine receptor in isolated identified neurones of Lymnaea stagnalis. *British Journal of Pharmacology , 115*, 275-282.

Mhuircheartaigh, R., Rosenorn-Lanng, D., Wise, R., Jbabdi, S., Rogers, R., & Tracey, I. (2010). Cortical and subcortical connectivity changes during decreasing levels of consciousness in humans: A functional magnetic resonance imaging study using propofol. *The Journal of Neuroscience , 30* (27), 9095-9102.

Multi Channel Systems MCS GmbH. (2005). *Microelectrode Array (MEA) User Manual.* Reutlingen, Germany: Multi Channel Systems MCS GmbH.

Nakagawa, I., idaka, S., Okada, H., Kubo, T., Okamura, K., & Kato, T. (2006). Effects of sevoflurane and propofol on evoked potentials during neurosurgical anesthesia. *Masui , 55* (6), 692-698.

Ng, Y., Chan, H., To, C., & Yap, M. (2008). The characteristics of multifocal electroretinogram in isolated perfused porcine eye cellular contributions to the in vitro porcine mfERG. *Documenta Ophthalmologica , 117*, 205-214.

Odom, J., Bach, M., Barber, C., Brigell, M., Marmor, M., Tormene, A., et al. (2004). Visual evoked potentials standard. *Documenta Ophthalmologica , 108*, 115–123.
O'Shea, S., Wong, L., & Harrison, N. (2000). Propofol increases agonist efficacy at the GABAA receptor. *Brain Research , 852*, 344-348.

Osterberg, G. (1935). Topography of the layers of rods and cones in the human retina. *Acta Ophthalmologica , 6(suppl.)*, 1-103.

OuYang, W., & Hemmings, H. (2007). Isoform-selective effects of isoflurane on voltage-gated Na+ channels. *Anesthesiology , 107*, 91-98.
Pocock, G., & Richards, C. (1993). Excitatory and inhibitory synaptic mechanisms in anaesthesia. *British Journal of Anaesthesia , 71*, 134-147.

Racine, J., Behn, D., & Lachapelle, P. (2008). Structural and functional maturation of the retina of the albino Hartley guinea pig. *Documenta Ophthalmologica , 117*, 13.

Racine, J., Joly, S., Rufiange, M., Rosolen, S., Casanova, C., & Lachapelle, P. (2005). The photopic ERG of the albino guinea pig (Cavia porcellus): A model of the human photopic ERG. *Documenta Ophthalmologica , 110*, 67.

Remington, L. (2005). *Clinical anatomy of the visual system* (2nd Edition ed.). St. Louis: Elsevier.

Ryu, S., Ye, J., Lee, J., Goo, Y., Kim, C., & Kim, K. (2009). Electrically-evoked neural activities of rd1 mice retinal ganglion. *The Korean Journal of Physiology & Pharmacology , 13*, 443－448.

Shibakawa, Y., Sasaki, Y., Goshima, Y., Echigo, N., Kamiya, Y., Kurahashi, K., et al. (2005). Effects of ketamine and propofol on inflammatory responses of primary glial cell cultures stimulated with lipopolysaccharide. *British Journal of Anaesthesia , 95* (6), 803-810.

Shiells, R., & Falk, G. (1990). Glutamate receptors of rod bipolar cells are linked to a cyclic GMP cascade via a G-protein. *Proceedings: Biological Sciences , 242* (1304), 91-94.

Sloan, T., Sloan, H., & Rogers, J. (2010). Nitrous oxide and isoflurane are synergistic with respect to amplitude and latency effects of sensory evoked potentials. *Journal of clinical monitoring and computing , 24*, 113-123.

Solovei, I., Kreysing, M., Lanctot, C., Kosem, S., Peichi, L., Cremer, T., et al. (2009). Nuclear architecture of rod photoreceptor cells adapts to vision in mammalian evolution. *Cell , 137* (2), 356-368.

Solt, K., & Forman, S. (2007). Correlating the clinical actions and molecular mechanisms of general anesthetics. *Current Opinion in Anaesthesiology , 20*, 300-306.

Stachnik, J. (2006). Inhaled anesthtic agents. *American Journal of Health-System Pharmacy , 63*, 623-634.

Stein, C. (1995). The control of pain in peripheral tissue by opioids. *The New England Journal of Medicine , 332*, 1685-1690.

Stoelting, R. (1999). *Pharmacology & Physiology in Anesthetic Practice* (3rd Edition ed.). Philadelphia: Lippincott Williams & Wilkins.
Susta, M., Stirn-Kranjc, B., Hawlina, M., & Brecelj, J. (2008). Photopic ON- and OFF-responses in complete type of congenital stationary night blindness in relation to stimulus intensity. *Documenta Ophthalmologica , 117*, 37-46.

Tanskanen, P., Kylma, T., Kommonen, B., & Karhunen, U. (1996). Propofol influences the electroretinogram to a lesser degree than thiopentone. *Acta Anaesthesiologica Scandinavica , 40*, 480-485.

Tashiro, C., Muranishi, R., Gomyo, I., Mashimo, T., Tomi, K., & Yoshiya, I. (1986). Electroretinogram as a possible monitor of anesthetic depth. *Graefe's Archive for Clinical and Experimental Ophthalmology , 224* (5), 473-476.

Thornton, C., Konieczko, K., Knight, A., Kaul, B., Jones, J., Dore, C., et al. (1989). Effect of propofol on the auditory evoked response and oesophageal contractility. *British Journal of Anaesthesia , 63*, 411-417.

Tootle, J. (1993). Early postnatal development of visual function in ganglion cells of the cat retina. *Journal of Neurophysiology , 69* (5), 1645-1960.

Trapani, G., Lopedota, A., Franco, M., Latrofa, A., & Liso, G. (1996). Effect of 2-hydroxypropyl-B-cyclodextrin on the aqueous solubility of the anaesthetic propofol (2, 6-diisopropylphenol). *International Journal of Pharmaceutics , 139*, 215-218.

Tremblay, F., & Parkinson, J. (2003). Alteration of electroretinographic recordings when performed under sedation or halogenate anesthesia in a pediatric population. *Documenta Ophthalmologica , 107*, 271-279.

Urban, B. (2002). Current assessment of targets and theories of anesthesia. *British Journal of Anaesthesia , 89* (1), 167-183.

Urban, B., & Bleckwenn, M. (2002). Concepts and correlations relevant to general anesthesia . *British Journal of Anesthesia , 89* (1), 3-16.

Vanlersberghe, C., & Camu, F. (2008). Etomidate and other non-barbiturates. *Handbook of experimental pharmacology , 182*, 267-282.

Vanlersberghe, C., & Camu, F. (2008). Propofol. *Handbook of Experimental Pharmacology , 182*, 227-252.

Vasileiou, I., Xanthos, T., Koudouna, E., Perrea, D., Klonaris, C., Katsargyris, A., et al. (2009). Propofol: A review of its non-anaesthetic effects. *European Journal of Pharmacology , 605*, 1-8.

Ver Hoeve, J., Danilov, Y., Kim, C., & Spear, P. (1999). VEP and PERG acuity in anesthetized young adult rhesus monkeys. *Visual Neuroscience , 16*, 607-617.
Wachtmeister, L. (1998). Oscillatory potentials in the retina: what do they reveal. *Progess in Retinal and Eye Research , 17* (4), 485-521.

Wali, N., & Leguire, L. (1992). The photopic hill: A new phenomenon of the light adapted electroretinogram. *Documenta Ophthalmologica , 80*, 335-342.

Westheimer, G. (2007). The ON-OFF dichotomy in visual processing: From receptors to perception. *Progress in Retinal and Eye Research , 26*, 636-648.

Widmaier, E., Raff, H., & Strang, K. (2004). *Vander, Sherman & Luciano's Human Physiology The Mechanisms of Body Functions* (9th Edition ed.). New York: The McGraw-Hill Companies.

Winkler, B. (1972). The electroretinogram of the isolated rat retina. *Vision Research , 12*, 1183-1198.

Wongpichedchai, S., Hansen, R., Koda, B., Gudas, V., & Fulton, A. (1992). Effects of halothane on childrens electroretinograms. *Ophthalmology , 99* (8), 1309-1312.

Woodward, W., Choi, D., Grose, J., Malmin, B., Hurst, S., Pang, J., et al. (2007). Isoflurane is an effective alternative to ketamine /xylazine/acepromazine as an anesthetic agent for the mouse electrogram. *Documenta Opthalmologica , 115*, 187-201.

Yu, D.-Y., Cringle, S., Alder, V., Su, E.-N., & Yu, P. (1996). Intraretinal oxygen distribution and choroidal regulation in the avascular retina of guinea pigs. *Amerian Journal of Physiology , 270* (39), H965-H973.